

## RESEARCH ARTICLE | *Control of Coordinated Movements*

# Corrective response times in a coordinated eye-head-arm countermanding task

Gordon Tao,<sup>1,2,3</sup> Aarlenne Z. Khan,<sup>2,4</sup> and Gunnar Blohm<sup>1,2,3</sup>

<sup>1</sup>Centre for Neuroscience Studies, Queen's University, Kingston, Ontario, Canada; <sup>2</sup>Canadian Action and Perception Network (CAPnet); <sup>3</sup>Association for Canadian Neuroinformatics and Computational Neuroscience (CNCN); and <sup>4</sup>School of Optometry, University of Montreal, Montreal, Quebec, Canada

Submitted 19 June 2017; accepted in final form 16 February 2018

**Tao G, Khan AZ, Blohm G.** Corrective response times in a coordinated eye-head-arm countermanding task. *J Neurophysiol* 119: 2036–2051, 2018. First published February 21, 2018; doi:10.1152/jn.00460.2017.—Inhibition of motor responses has been described as a race between two competing decision processes of motor initiation and inhibition, which manifest as the reaction time (RT) and the stop signal reaction time (SSRT); in the case where motor initiation wins out over inhibition, an erroneous movement occurs that usually needs to be corrected, leading to corrective response times (CRTs). Here we used a combined eye-head-arm movement countermanding task to investigate the mechanisms governing multiple effector coordination and the timing of corrective responses. We found a high degree of correlation between effector response times for RT, SSRT, and CRT, suggesting that decision processes are strongly dependent across effectors. To gain further insight into the mechanisms underlying CRTs, we tested multiple models to describe the distribution of RTs, SSRTs, and CRTs. The best-ranked model (according to 3 information criteria) extends the LATER race model governing RTs and SSRTs, whereby a second motor initiation process triggers the corrective response (CRT) only after the inhibition process completes in an expedited fashion. Our model suggests that the neural processing underpinning a failed decision has a residual effect on subsequent actions.

**NEW & NOTEWORTHY** Failure to inhibit erroneous movements typically results in corrective movements. For coordinated eye-head-hand movements we show that corrective movements are only initiated after the erroneous movement cancellation signal has reached a decision threshold in an accelerated fashion.

decision making; error correction; LATER model; pointing; saccade

## INTRODUCTION

Making mistakes is an everyday phenomenon. When erroneously initiating or performing movements, it can be crucial to correct them as quickly as possible. For example, in sports, when challenging an opposing player in soccer, hockey, or basketball one may have to respond quickly to a feint, where the opponent motions in one direction and then suddenly changes direction, by canceling one's initial reaction and responding to the new information. The mechanisms underlying corrective response initiation as well as the coordination of multiple effectors in this context remain unclear. To gain

insight into potential mechanisms governing corrective response initiation, we investigated corrective response times (CRTs) in a coordinated eye, head, and arm countermanding task.

Our research question is couched in the framework of response inhibition. Response inhibition refers to the suppression of voluntary actions that are no longer desired, for example, pulling a swing in baseball. Response inhibition (Coe and Munoz 2017; Cutsuridis 2017; Noorani 2017; Noorani and Carpenter 2016; Pouget et al. 2017; Schall et al. 2017; Song 2017) has been widely explored with behavioral tasks (Beuk et al. 2014; Hanes and Carpenter 1999; Hanes and Schall 1995; Khan et al. 2015; Noorani and Carpenter 2013; Salinas and Stanford 2013; Schall and Godlove 2012; Stevenson et al. 2009), neurophysiological methods (Jantz et al. 2013; Nyffeler et al. 2007; Pouget et al. 2011; Ray et al. 2009b; Stuphorn and Schall 2006), and functional imaging (Domagalik et al. 2012; Mattia et al. 2012; Hakvoort-Schwerdtfeger et al. 2012). Implicated neural substrates include the superior colliculus (Paré and Hanes 2003), frontal eye fields (Hanes et al. 1998; Ramakrishnan et al. 2012), inferior frontal gyrus, basal ganglia, and supplementary motor area (Aron 2007; Chambers et al. 2009). In populations with conditions such as Parkinson disease and attention deficit/hyperactivity disorder, response inhibition and its underlying neural substrates have been shown to be altered (Chambers et al. 2009; Cutsuridis 2017; Groman et al. 2009; Ray et al. 2009a; Verbruggen and Logan 2009).

A common approach to explicitly test inhibition of prepared responses is through the stop-signal paradigm (Hanes and Carpenter 1999; Hanes and Schall 1995; Logan and Cowan 1984). In this paradigm, participants are asked to perform a motor task, such as pressing a button, upon presentation of a Go signal. On a small proportion of trials, a Stop signal is presented, which instructs participants to inhibit and cancel the impending motor response. Depending on the delay of the Stop signal after the Go signal, the trial would result in either stop-success or stop-failure, with higher proportions of stop-failure trials corresponding to longer stop-signal delays (SSDs).

Response inhibition performance has been classically described with a race-to-threshold model (Boucher et al. 2007; Cutsuridis 2017; Noorani 2017; Noorani and Carpenter 2013), originally proposed by Logan and Cowan (1984). Each racing decision alternative has typically been modeled with a linear approach to threshold with ergodic rate (LATER) process, first

Address for reprint requests and other correspondence: G. Blohm, Queen's Univ., Centre for Neuroscience Studies, Botterell Hall, Rm. 229, 18 Stuart St., Kingston, ON K7L 3N6, Canada (e-mail: gunnar.blohm@queensu.ca).

developed by Carpenter (Carpenter 1981; Reddi and Carpenter 2000). The model describes the performance as the outcome of a race to threshold between a Go and a Stop process, two independent and stochastic processes. The Go process is triggered by the target and initiates the response when it reaches threshold, corresponding to the reaction time (RT). The Stop process is triggered by the Stop signal and inhibits the response only if it reaches threshold before the Go signal. The latency of the Stop process reaching threshold is defined as the stop signal reaction time (SSRT) and represents the performance quantifier of response inhibition. Since the SSRT cannot be directly observed, it must be estimated through the proportions of stop-success trials at different SSDs. Thus the race model provides a basic mechanism that explains how we are able to stop ourselves from making erroneous actions.

In the case of an error, the Go signal reaches threshold before the Stop process, which results in an erroneous response that requires correction. Under the response inhibition framework, corrective responses may be viewed as an adaptive action to the failed response inhibition. To date, investigation of the mechanisms involved in the initiation of corrective responses in response to error has been limited. While corrective responses have been observed with a countermanding paradigm (Corneil and Elsley 2005), they were not explicitly prompted and their latencies were not analyzed. Other studies have utilized slightly different paradigms, such as the stop-change and double-step tasks, which explicitly required the participant to perform a second motor task upon Stop signal presentation (Verbruggen and Logan 2008a, 2009); however, these secondary responses are not corrective responses per se as they were not driven by errors. One recent study investigated corrective saccade initiation during an antisaccade task (Noorani and Carpenter 2014) using an extension of the LATER model. Their results suggest that multiple sequential decisions take place for movement initiation and correction.

We investigated initiation, inhibition, and corrective responses of multiple effectors to understand decision processes during coordinated actions. Many studies have demonstrated strong correlations of motor initiation times between the eye and head (Biguer et al. 1982; Corneil and Elsley 2005; Guitton et al. 1990; Khan et al. 2009), between the eye and arm (Carey 2000; Dean et al. 2011; Fischer and Rogal 1986; Fisk and Goodale 1985; Gribble et al. 2002; Herman et al. 1981; Jeannerod 1988), and between all three effectors (Suzuki et al. 2008). However, others have found little or no correlation (Guitton and Volle 1987; Phillips et al. 1995; Tweed et al. 1995; Vercher et al. 1994), particularly between head and arm movement initiation (Vercher et al. 1994). Thus there is yet no consensus as to the degree of coupling between multiple effector initiation processes (Dean et al. 2011; Freedman and Sparks 2000). In addition, the coupling between corrective responses of different effectors has been little investigated (Boucher et al. 2007; Corneil and Elsley 2005), and the few studies mentioned here have utilized only paired effectors (eye and hand or eye and head). The present study uses a gaze shift and pointing task to investigate initiation, inhibition, and corrective responses during combined eye-head-arm movements. This work has been previously published in abstract format (Tao and Blohm 2011).

## METHODS

### *Participants*

Seven healthy participants (aged 21–29 yr; 6 men, 1 woman) participated in this experiment, and each provided informed written consent. Six participants were naive to the goals of the study. All participants had normal or corrected-to-normal vision and had no history of neurological disease. Experimental procedures were approved by the Queen's University Research Ethics Board in compliance with the Declaration of Helsinki.

### *Experimental Setup*

Participants were seated upright in a dark room with no background illumination. The participant's preferred (dominant) arm was suspended with a sling such that it was relaxed, straight, and parallel to the ground. The arm sling was used throughout the experiment both to prevent fatigue of the arm and to avoid muscle activation due to gravity. At 1 m directly in front of the participant, we positioned a horizontal array of light-emitting diodes (LEDs) raised to the level of the arm. A green fixation LED was centered directly in front of the participant, with two green target LEDs at 30° to either side of the participant's forward gaze. A red LED was stacked 5 mm on top of the fixation LED and served as the Stop signal in our countermanding task.

Movements in the horizontal axis of both eyes were measured with a head-mounted Chronos Eye Tracking Device (Chronos Vision, Berlin, Germany) at 400 Hz with errors <0.1°. Head and arm movements were recorded with active infrared markers that were tracked in three-dimensional space with an Optotrak motion capture system (NDI, Waterloo, ON, Canada) at 400 Hz. Markers were placed on the finger, elbow, and shoulder and on the head-mounted eye tracker in a triangular plane to measure head movements. In addition to kinematic measures, we also recorded muscle EMG activity for head and arm movements. For head movements, the sternocleidomastoid and trapezius muscles were recorded bilaterally as previously done (Khan et al. 2009). For arm movements, activities of the anterior deltoid, lateral deltoid, posterior deltoid, and pectoralis major muscles were measured (Pruszynski et al. 2010). Activity in each muscle was recorded with DE-2.1 (Delsys, Boston, MA) single differential surface electrodes (1 electrode per muscle) connected to a Bangoli Desktop EMG system (Delsys) at 1 kHz. These muscles were selected for their accessibility and do not constitute all of the muscles involved in the movements. Muscles in the splenius, longissimus, and longus groups also contribute to head rotation, while other muscles in the pectoral girdle such as the subscapularis and teres major and minor contribute to the tasked arm movements. However, these muscles lie much deeper and cannot be easily recorded with surface electrodes. Thus we did not necessarily measure the first muscles recruited during the effector movements (Corneil et al. 2002; Goonetilleke et al. 2015).

### *Task*

We utilized a countermanding paradigm that has been widely used to explore response inhibition (Verbruggen and Logan 2008b). In the task (Fig. 1), participants were required to maintain central gaze with the head oriented and the arm pointing at a central fixation point. On Go trials, a visual target (Go signal) presented on either side of the fixation point prompted participants to perform the motor task: orienting their gaze (eyes and head) and arm to the target as quickly as possible. Occasionally, a Stop signal instructing the participant to withhold the response followed the Go signal after a specific SSD. In this situation, the participant would either successfully withhold the response or produce a response, depending on whether the countermanding task was successful or not. In the specific case of stop-failure, participants were instructed to reorient all effectors to the central fixation point as quickly as possible. We emphasized the

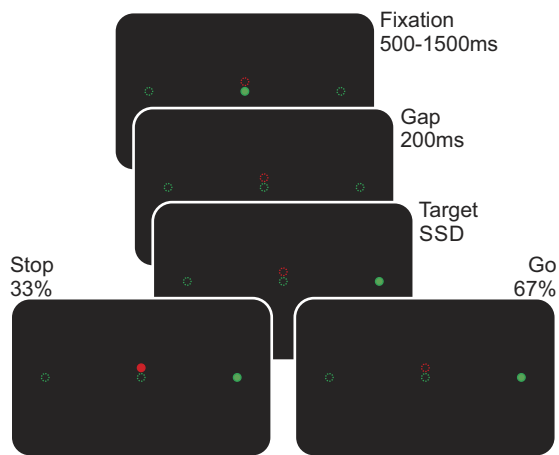


Fig. 1. All trials began with a 500- to 1,500-ms central green fixation LED. After a 200-ms gap, a green target LED was presented 30° to either the left or right of fixation. In 67% of trials (Go condition), the target LED stayed illuminated until the end of the trial (1,500 ms). In 33% of trials (Stop condition), a red central LED was illuminated after a random Stop signal delay (25, 75, 125, 175, or 225 ms) after the target appeared in addition to the target LED. Participants were instructed to inhibit their movement toward the target or to return to the central Stop signal if they failed to inhibit their response.

importance of maintaining a natural response without strategizing future responses. Participants performed a number of practice trials until they felt comfortable with the procedure.

The experiment consisted of 67% Go trials, where the target was presented without the Stop signal, randomly interspersed with the remaining 33% of Stop trials. Trials began with gaze centered on and arm pointing at a green central fixation point for a random duration between 500 and 1,500 ms, after which the fixation point was extinguished. Then, one of the two green targets (30° left or right) was presented after a 200-ms delay. The eccentricity of the target was chosen to be sufficiently large such that head movements naturally accompanied saccades. The 200-ms delay was primarily used to distinguish the Stop signal at very short SSDs from the fixation point; the delay also disinhibits fixation and results in an expediting effect on RTs (gap effect) in the eye (Munoz and Fecteau 2002; Stevenson et al. 2009), head (Corneil and Munoz 1999), and arm (Bekkering et al. 1996). Targets appeared randomly with equal probability on either the left or right. During 33% of trials, the central red LED was illuminated after a variable SSD (randomly drawn from 25, 75, 125, 175, and 225 ms) for 1,500 ms. Trials were identified as Go, Stop (successful stop trials), or corrected (unsuccessful stop trials) trials. Target LEDs remained on for the duration of the SSD and Stop signal presentation (if applicable). During the intertrial interval, all LEDs were turned off for 2 s, and participants were instructed to return to the center fixation position. All participants performed a total of 1,200 trials in 50 trial blocks over two sessions, except for two participants who completed only 1,000 and 1,150 trials, respectively, and one participant who completed an additional block for a total of 1,250 trials.

#### Data Analysis

Data were analyzed off-line with MATLAB (MathWorks, Natick, MA). Eye (saccades), head, and arm movements were automatically detected and corrected by visual inspection as needed. Right eye movement data were low-pass filtered with an autoregressive forward-backward filter with a cutoff frequency of 50 Hz. Eye velocity and acceleration were obtained by differentiation via a central difference algorithm. Saccades were detected when eye acceleration first exceeded a threshold of 1,000°/s<sup>2</sup> after target onset.

Orientation and position of the head and arm were determined in three-dimensional space based on markers placed on the eye tracker (3

in a triangle), the shoulder, elbow, and finger, with the rotational reference point converted from the fixation-point centered position. These data were also low-pass filtered with an autoregressive forward-backward filter with a cutoff frequency of 25 Hz. Velocity and acceleration were obtained by differentiation via central difference algorithm. Onsets of head and arm movements were detected using a threshold of 200°/s<sup>2</sup> acceleration. In addition to the kinematic measures, the onsets of head and arm movements were also detected from the EMG activity of the muscles with a variable-threshold algorithm. EMG signals were band-pass filtered off-line (15–350 Hz) and full-wave rectified. Signal noise before the start of each trial was used to estimate the baseline EMG amplitude.

RTs were determined by the kinematic movement onset and EMG onset in each effector. EMG RT was defined as the onset of muscle activity following target presentation of the first of all agonist muscles. Muscle activity onset was set as the time at which there was a consistent rise above baseline amplitude [3 standard deviations (SDs)].

Participants made 100% corrective responses on failed trials; they were explicitly instructed to correct any errors. On corrective trials, responses to the Stop signal were quantified as the time between the Stop signal and the onset of the corrective response: CRT. CRTs were defined as the time at which movements began in the direction opposite to the initial movement. EMG CRT was based on the earliest muscle activity onset of the antagonist muscles, given that there was a corresponding corrective movement in the kinematics. For these trials, CRT was determined by using kinematic onset as a region of interest guide for marking EMG onset within the single burst.

#### Modeling

We took a stepwise model fitting approach during which we first determined the Go process parameters according to the LATER model, then fitted a dual process (Go and Stop) race model (Cutsuridis 2017) to the inhibition function to determine Stop process parameters, and finally used these model parameters as the basis for modeling CRT data.

*Modeling the Go process: LATER.* Motor RTs have been described by the LATER model developed by Carpenter (Carpenter 1981; Reddi and Carpenter 2000). According to the LATER model, movement is initiated when a linearly rising signal, in response to the Go stimulus, reaches threshold. The rate of rise of the LATER process is normally distributed, and the RTs are related to the rate such that

$$T = \frac{(S_T - S_0)}{r}$$

where  $T$  is the reaction time,  $r$  is the rate,  $S_0$  is the resting level, and  $S_T$  is the threshold. For the purposes of our model,  $(S_T - S_0) = 1$  and therefore

$$r = 1/T$$

Since  $r$  follows a normal distribution,  $T$  may be said to follow a reciprocal normal, or recinormal, distribution. This LATER process was used to model the Go RT distribution for each participant's effector (eye, head, arm) according to the probability density function (PDF) with rate parameters  $\mu_r$  and  $\sigma_r$ :

$$f(T|\mu_r, \sigma_r) = \begin{cases} \frac{1}{T^2 \sqrt{2\pi\sigma_r^2}} e^{-\frac{(1 - \mu_r T)^2}{2\sigma_r^2 T^2}} & \text{if } T > 0 \\ 0 & \text{elsewhere} \end{cases}$$

*Computing the inhibition function.* According to the race model proposed by Logan and Cowan (1984), inhibition performance is dependent on the relative finishing times of two competing races, i.e., the Go process and the Stop process. However, the Stop process cannot be directly measured and must be inferred from the inhibition

function (i.e., Stop trial performance as a function of SSD) of Stop trials; the inhibition function describes the probability of responding to the Go signal over the range of SSDs. To compute the inhibition function, we used a numerical approach to integrate the joint PDFs of two LATER processes, Go and Stop, that determines the race outcome (Logan and Cowan 1984) such that

$$p(T_{Go}|T_{Stop+SSD}) = \int_0^{\infty} p(T_{Go}|T_{Stop+SSD,i}) \cdot p(T_{Stop+SSD,i}) \cdot dT_{Stop+SSD,i}$$

with

$$p(T_{Go}|T_{Stop+SSD,i}) = \begin{cases} p(T_{Go}) & \text{if } T_{Go} < T_{Stop+SSD,i} \\ 0 & \text{if } T_{Go} > T_{Stop+SSD,i} \end{cases}$$

where  $T_{Go}$  and  $T_{Stop+SSD,i}$  are the reclinormal PDFs of the Go process and the Stop process respectively, with rate parameters  $\mu_{r(Go)}$ ,  $\sigma_{r(Go)}$ ,  $\mu_{r(Stop)}$ , and  $\sigma_{r(Stop)}$ .

$$p(T_{Stop+SSD,i}) = f_{Stop}(T|\mu_r, \sigma_r)$$

and

$$p(T_{Go}) = f_{Go}(T|\mu_r, \sigma_r)$$

Therefore, the inhibition function may be modeled according to

$$p(\text{Response}|\text{Stop signal}) = \frac{p(T_{Go}|T_{Stop+SSD})}{p(T_{Go})}$$

$T_{Go}$  was defined by the PDF of the corresponding participant-effector Go RT model. We fit the modeled inhibition function via nonlinear regression with iterative least squares estimation to estimate the rate parameters  $\mu_{r(Stop)}$  and  $\sigma_{r(Stop)}$  of the Stop process.

**Modeling corrective response time.** Models for the CRT distributions were built upon the above race model. We took an exploratory approach to constructing these models, beginning with the fewest additional parameters possible. Some models (see RESULTS) included a second Go process for the corrective movement that was also modeled by an independent LATER process. Models were fit to the joint cumulative distribution function of the race model via nonlinear regression with iterative least squares estimation. Models that were not obviously invalid (i.e., could not fit the data) were compared quantitatively using three information criteria: the Bayesian information criterion (BIC), the Akaike information criterion (AIC), and the Hannan-Quinn information criterion (HQC). Each criterion for model selection penalizes the trade-off between goodness of fit and model complexity differently. To evaluate confidence of model selection, we then estimated the probability of a given model minimizing the estimated loss of information (Burnham and Anderson 2003) as

$$p(\text{correct model}) = e^{\frac{\min\langle C \rangle - C_i}{2}}$$

where  $C$  is the list of information criterion measures of each model for a given criterion and  $C_i$  stands for an individual measure. This relative likelihood of models was evaluated separately for different effectors and kinematic/EMG data.

## RESULTS

We collected data from 8,200 trials across all seven participants, out of which 931 trials were excluded because of errors in eye movement recording or errors made by the participant (e.g., unsatisfactory fixation at trial start). Recordings for two participants were incomplete; EMG data for *S6* and *S7* were too noisy to reliably capture movement-related activity for a large proportion of trials. For these participants, kinematic data were used in place of EMG data. Furthermore, eye position data could not be reliably extracted from the video images for

*S7* because of drooping eyelids. Therefore, these data were excluded from analysis.

Figure 2 illustrates example recordings from two individual failed Stop signal trials in which the participant failed to cancel the planned movement and carried out a corrective return movement. Figure 2A shows an example in which Go and corrective return movements occurred sequentially, while Fig. 2B shows an example of interrupted Go movement during which the return movement began before the Go movement ended. Kinematic data (Fig. 2, left) show different movement times for eyes, head, and arm. This is supplemented by EMG recordings (Fig. 2, right) for eight different muscles, also showing different head and arm onset times. In Fig. 2A, corrective movements back to the center LED can be observed later in the trial and were initiated by muscle groups opposite to the initial movements (which were also involved in braking movements for the initial movement). In Fig. 2B, these braking movements blend with the initiation of the return movement.

In the following sections, we perform a stepwise analysis to evaluate the different response components, i.e., Go process parameters, Stop process properties, and CRTs. Thus we first describe the Go RTs and their correlation across effectors. We then use the Stop trials to evaluate the response inhibition function and associated LATER processes for each effector. Finally, we use this information to constrain potential models capturing the CRTs and compare CRT properties across effectors.

### RT Analysis

On Go trials, participants responded to the target stimulus by making an eye-head-arm movement toward it. For each participant, five RT distributions were calculated: eye RTs were determined from motion tracking while head and arm RTs were determined from both motion tracking and EMG (see METHODS). Mean RTs ranged from 186 ms to 328 ms across participants (Table 1). As expected, kinematic onset was consistently measured after EMG onset, and the two were tightly correlated (Fig. 3, A and B).

Coordination of the kinematic RTs on Go trials were evaluated with partial correlation analysis (Fig. 3C) across six participants (*S1–S6*). The eye and head showed the strongest relationship, with a partial correlation coefficient of  $\rho_{EH-A} = 0.724$  (pooled data) and ranging from 0.559 to 0.884 for individual participants. The head-arm pair showed a weaker relationship, with a coefficient of  $\rho_{HA-E} = 0.306$  (range for individual participants = 0.369–0.787). The weakest relationship was observed for the eye-arm pair, with a coefficient of  $\rho_{EA-H} = 0.303$  (–0.138 to 0.297). Note that because the data were pooled rather than averaged, they could differ from the individual ranges. These results were corroborated using covariance derived from mixed model analysis (not shown), in terms of overall relative strength of relationships. These findings demonstrate that movement decisions for individual effectors are not independent but at least partially linked, in agreement with the literature (Boucher et al. 2007; Corneil and Elsley 2005; Dean et al. 2011).

The first part of our iterative model fitting procedure was to evaluate the Go process. Distributions of Go RTs were well fitted with a reclinormal distribution (Fig. 4) described by the LATER model. The individual fit parameters of arm and head

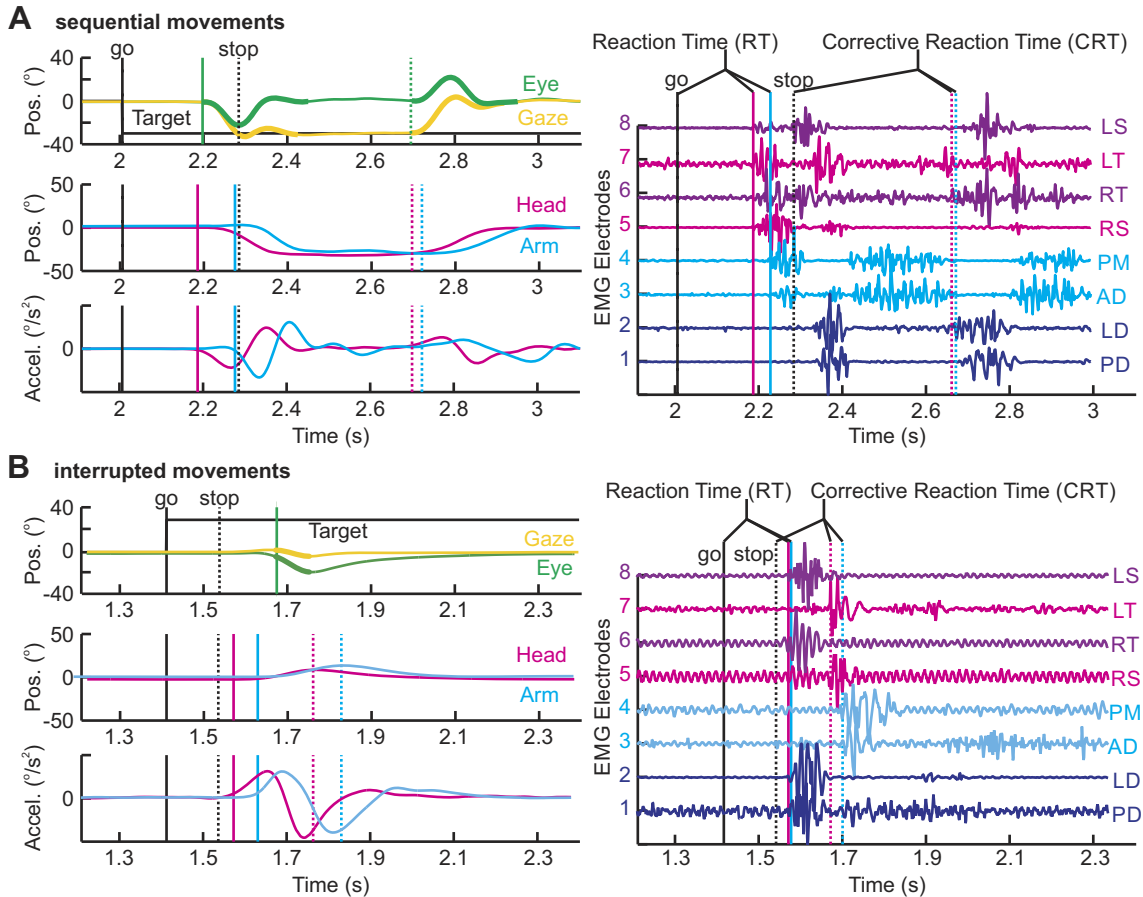


Fig. 2. Typical failed Stop trials. *A*: example data from a Stop trial with sequential Go and corrective return movements, with Go signal (vertical solid black line), Stop signal (vertical dotted black line), and corresponding reaction times (vertical solid colored lines) and corrective response times (vertical dotted colored lines). *Top left*: position (°) of the eye and head + eye = gaze with saccades denoted by bolded lines. *Bottom left*: position and acceleration (°/s<sup>2</sup>) of the head and arm are shown with the kinematic response initiation time (vertical solid colored lines) and kinematic corrective response initiation time (vertical dotted colored lines). *Right*: EMG data from the neck (magenta/violet) and arm muscles (blue/indigo). For this target, *traces 3, 4, 5, and 7* govern responses and *traces 1, 2, 6, and 8* govern corrective responses. Head movements were recorded from left/right sternocleidomastoid (LS, RS) and trapezius (LT, RT) muscles. Arm movements were recorded from anterior deltoid (AD), lateral deltoid (LD), posterior deltoid (PD), and pectoralis major (PM) muscles. *B*: typical interrupted Stop trial in which the corrective arm and head return movements occurred before the end of the Go movement. Note that the opposite direction eye saccade compensates for the (erroneous) head movement.

distributions are shown in Table 2 and were subsequently used to estimate the SSRT.

*Response Inhibition*

Of the 2,592 Stop trials, 2,457 trials were kept for further analysis (135 were discarded because of error or problems in eye/head/arm movement recordings). Of those, 1,112 trials (45% of all Stop trials) showed complete inhibition of the

motor response, i.e., all effectors were successfully inhibited, while 985 (38%) trials showed unsuccessful inhibition (stop-failures) for all three effectors. Overall, this is indicative of mostly dependent decision processes, as all three effectors moved or did not move together for 83% of all Stop trials. In addition, some trials showed partially independent responses whereby one or two effectors were successfully inhibited while others initiated a motor response (17% of trials; Table 3),

Table 1. Reaction times on Go trials

	S1	S2	S3	S4	S5	S6	S7
KIN eye	218 ± 45	250 ± 53	187 ± 57	304 ± 55	271 ± 57	225 ± 33	
KIN head	203 ± 45	257 ± 52	218 ± 57	283 ± 55	288 ± 64	232 ± 38	248 ± 60
KIN arm	267 ± 49	254 ± 55	242 ± 59	328 ± 52	271 ± 61	278 ± 39	281 ± 57
EMG head	200 ± 46	231 ± 55	210 ± 57	278 ± 55	259 ± 65		
EMG arm	218 ± 48	214 ± 56	186 ± 59	283 ± 53	219 ± 62		
K-E head	3.0 ± 11	26 ± 20	8.0 ± 21	4.8 ± 11	29 ± 24		
K-E arm	49 ± 17	19 ± 18	21 ± 25	11 ± 14	24 ± 28		

Data (in ms) are presented as mean ± SD. KIN, kinematic data from motion tracking; EMG, electromyographic data; K-E, difference between kinematic and EMG latencies (KIN – EMG).

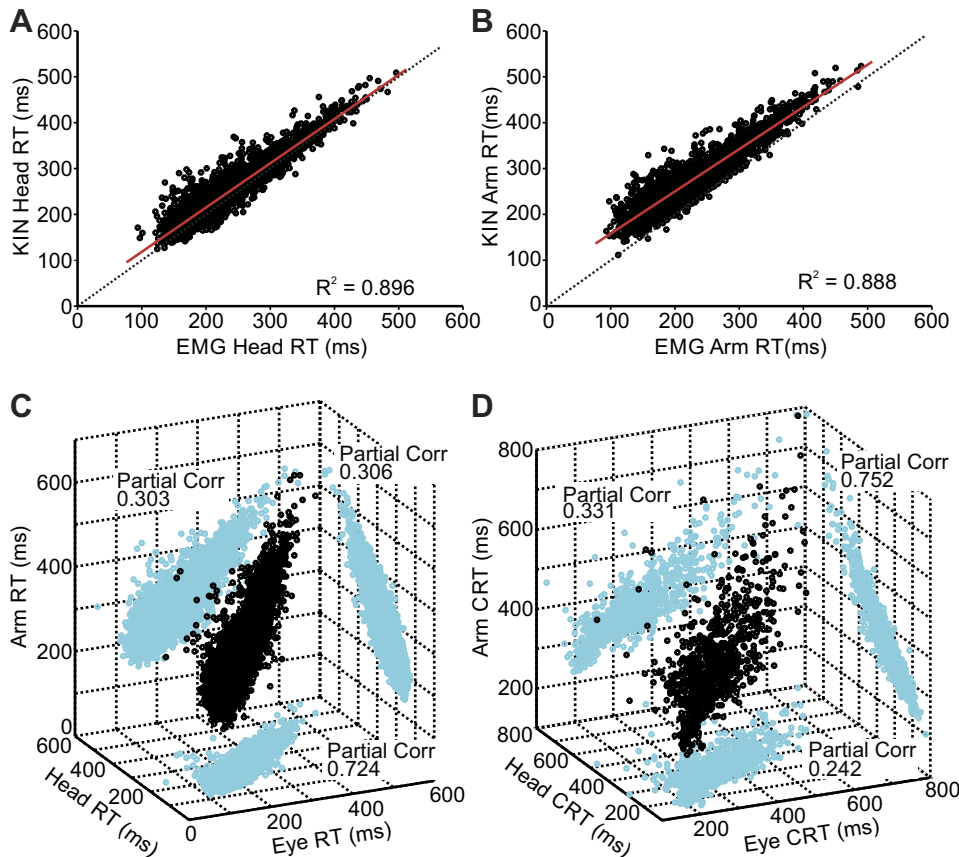


Fig. 3. EMG onset precedes kinematic onset as expected for Go response reaction times. *A*: head movements:  $R^2 = 0.896$ ,  $y = 0.966x + 22$  (red fit line). *B*: arm movements:  $R^2 = 0.888$ ,  $y = 0.921x + 66$ . Across all 7 participants; dotted line represents the line of unity. *C* and *D*: plot of Go RTs (*C*) and CRTs (*D*) for the 3 effectors (black); 2D projections (cyan) are shown for effector pairs with corresponding partial correlation coefficients. Correlational analysis was performed across 6 participants (*S1–S6*).

suggesting some partially independent decision processes across effectors. Therefore, we calculated the SSRT of each effector for each participant independently. Note that we excluded *participant S6* from all subsequent analyses because this participant generally failed to inhibit the response, resulting in too low a number of successful Stop trials to fit the inhibition function. The inhibition function (SSRT) shows the proportion of stop-failure as a function of SSD (Fig. 5), with a general trend of more stop-failure trials, i.e., fewer successful Stop trials, occurring with increased SSD. The SSRT pattern observed showed that Stop trials for arm movements (Fig. 5C) generally had the lowest inhibition rate (lowest successful Stop trial proportion), those for eye movements (Fig. 5A) had the highest inhibition rate, and head movements were intermediate (Fig. 5B).

To estimate the SSRT, we fit the mean rate and SD of the Stop process such that the outcome of our race model optimally matched the observed inhibition function. Mean SSRTs ranged from 50 ms to 183 ms across the different effectors (Fig. 6). Figure 6 shows that eye SSRTs were shortest, followed by head SSRTs and arm SSRTs being longest. The fitted Stop

process parameters define the respective SSRT recinormal distribution. Fit parameters and statistics for the SSRT estimates can be found in Table 2.

#### CRT Analysis

On failed Stop trials, participants returned effectors to the central fixation position as instructed (Fig. 2). As mentioned in METHODS, while head and arm movements tended to be interrupted midflight, this was generally not the case for eye movements; they tended to be completed and were followed shortly by the return movement. Thus our measure of the CRTs for the eyes was different from that of the head and arm. Nevertheless, we wished to calculate an estimate of the number of interrupted movements that was comparable across all three effectors, to determine the relationship between them. Processes triggering eye corrective responses are considered to remain covert until completion of the erroneous Go saccade. However, it is well known that competing motor goals can modify saccade end points (Becker and Jürgens 1979; Camalier et al. 2007; Chou et al. 1999; McPeck et al. 2003;

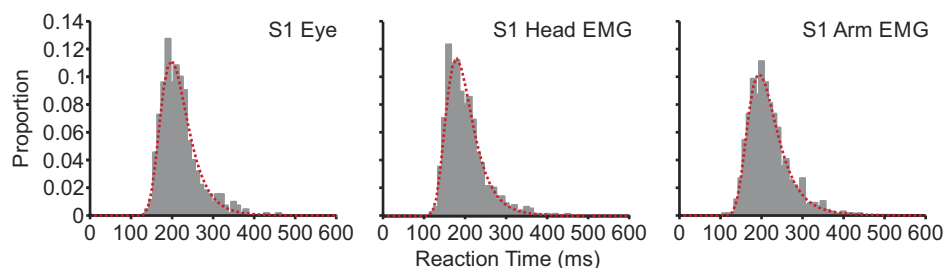


Fig. 4. Example RT distributions for the eye, head EMG, and arm EMG of *S1* on Go trials. *y*-Axis denotes the proportion of total trials; *x*-axis denotes the RTs for each effector (counted within 10-ms bins). The LATER model fit is overlaid as the red line.

Table 2. Summary of fitted race model parameters between RT and SSRT

	RT Parameter, s <sup>-1</sup>		K-S Test P Value	SSRT Parameter, s <sup>-1</sup>	95% CI
<i>S1</i>					
EMG head	$\mu_{\text{rate}}$	5.227	0.918	8.325	[7.450, 9.200]
	$\sigma_{\text{rate}}$	1.027		2.090	[0.334, 3.845]
EMG arm	$\mu_{\text{rate}}$	4.796	0.999	7.070	[6.421, 7.719]
	$\sigma_{\text{rate}}$	0.966		1.031	[-0.530, 2.592]
<i>S2</i>					
EMG head	$\mu_{\text{rate}}$	4.552	0.348	10.656	[8.568, 12.745]
	$\sigma_{\text{rate}}$	1.028		4.523	[0.170, 8.876]
EMG arm	$\mu_{\text{rate}}$	4.985	0.144	8.255	[7.104, 9.405]
	$\sigma_{\text{rate}}$	1.237		2.676	[-0.067, 5.419]
<i>S3</i>					
KIN head	$\mu_{\text{rate}}$	4.83	0.880	7.929	[6.374, 9.483]
	$\sigma_{\text{rate}}$	0.976		3.347	[-1.069, 7.763]
KIN arm	$\mu_{\text{rate}}$	4.330	0.980	5.636	[4.656, 6.617]
	$\sigma_{\text{rate}}$	0.855		0.970	[-2.307, 4.246]
<i>S4</i>					
EMG head	$\mu_{\text{rate}}$	3.737	0.107	9.208	[8.254, 10.162]
	$\sigma_{\text{rate}}$	0.745		4.627	[2.204, 7.050]
EMG arm	$\mu_{\text{rate}}$	3.658	0.257	7.765	[6.454, 9.076]
	$\sigma_{\text{rate}}$	0.698		3.646	[0.361, 6.931]
<i>S5</i>					
EMG head	$\mu_{\text{rate}}$	4.129	0.0981	10.043	[-0.854, 20.939]
	$\sigma_{\text{rate}}$	1.380		9.488	[-10.906, 29.881]
EMG arm	$\mu_{\text{rate}}$	4.939	0.320	8.562	[6.912, 10.212]
	$\sigma_{\text{rate}}$	1.380		2.240	[-1.205, 5.684]
<i>S7</i>					
KIN head	$\mu_{\text{rate}}$	4.225	0.217	10.583	[9.646, 11.520]
	$\sigma_{\text{rate}}$	0.842		4.085	[2.450, 5.721]
KIN arm	$\mu_{\text{rate}}$	3.683	0.649	6.370	[5.717, 7.022]
	$\sigma_{\text{rate}}$	0.684		1.794	[0.566, 3.022]

Parameters  $\mu_{\text{rate}}$  and  $\sigma_{\text{rate}}$  describe the normal rate distribution governing each process.

McPeck and Keller 2001; Minken et al. 1993). Thus we presumed that interrupted movements should lead to smaller amplitudes than noninterrupted movements for eye movements, and also for head and arm movements. We therefore compared initial movement amplitudes (toward the target) during failed Stop trials (with corrective movements back to center) to the initial movement amplitudes during Go trials (Fig. 7A). Figure 7A shows the differential frequency between the failed Stop and Go trials as a function of amplitude. As can be seen, there were more trials with smaller amplitudes and fewer trials with larger amplitudes during failed Stop trials

Table 3. Stop trial outcomes

	Eye	Head	Arm	Eye-Head	Eye-Arm	Head-Arm	NoneStop	AllStop
<i>S1</i>	40	0	0	14	9	0	135	148
<i>S2</i>	15	3	0	37	0	1	97	216
<i>S3</i>	5	5	0	21	0	3	204	95
<i>S4</i>	4	0	7	12	2	1	101	254
<i>S5</i>	11	1	0	62	0	2	98	194
<i>S6</i>	10	0	75	0	4	2	196	29
<i>S7</i>	26	3	0	28	0	0	111	176
Total	111	12	82	174	15	9	942	1112

Columns headed Eye, Head, and Arm show no. of trials where only the indicated effector was successfully inhibited (but not the other 2 effectors). Columns with paired effector headings show no. of trials with successful inhibition of the paired effectors (but not the third). Column headed NoneStop shows no. of trials where none of the effectors was successfully stopped (all 3 effectors initiated a movement). Column headed AllStop shows no. of trials where all 3 effectors were successfully inhibited. Only trial counts based on kinematics measures are shown; in some cases, an EMG response was present but no kinematic movement was detected.

compared with Go trials. The cutoffs for interrupted movements was defined as the zero-crossing of the differential histogram for the respective effectors, which allowed us to estimate the number of interrupted movements for saccades, head, and arm movements using identical criteria. Note that the pattern is very similar across the three effectors, considering that head and arm movements were interrupted midflight and eye movements tended not to be.

In Fig. 7B is shown the relative proportions of trials with interrupted movements across the three effectors. Consistent with previous findings, the biggest proportion of trials involved interruptions for all three effectors together (40%). The second biggest proportion were trials in which the arm and head were interrupted but not the eye (15%). A small number of trials involved interruptions for just one effector and not the other two (only arm interruptions = 9%, only head interruptions = 7%, only eye interruptions = 4%). These findings are very similar to those seen for successful Stop trials (Table 3), as can be seen in Fig. 7C, where successful Stop trials were included as well.

The proportion of partial responses was highly dependent on the SSD. As shown in Fig. 8, for short SSDs it was unlikely to find all effectors erroneously responding (None Stop) and far more likely to find all effectors being successfully countermanded (All Stop). This trend was reversed for long SSDs. Interestingly, partial inhibition of one or two of the three effectors was more frequently observed for intermediate SSDs (Fig. 8), similar to observations reported by Corneil and Elsley (2005). Thus the SSD had a large influence on the probability of observing particular partial responses/inhibition.

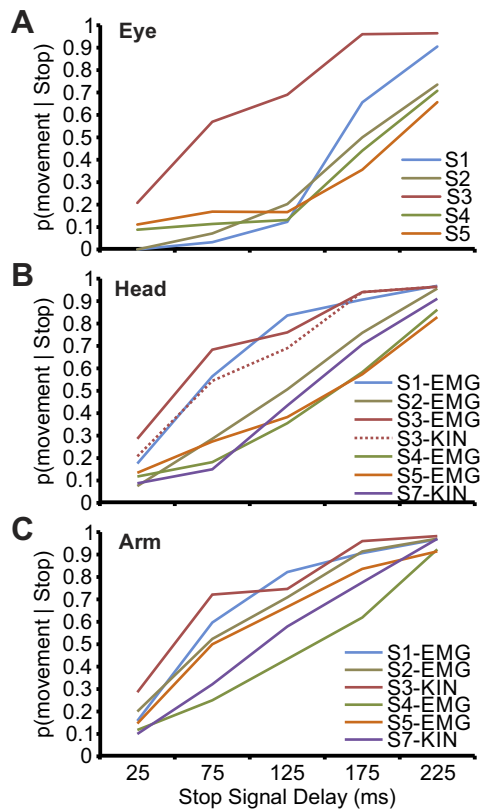


Fig. 5. Summary of observed inhibition functions. SSRTs were estimated by fitting the race model to each individual's inhibition functions separately for eye movements (A), head movements (B), and arm movements (C). Different colored lines represent different participants. For head (B) and arm (C) movements, both kinematic and EMG-based data are shown when available. Root mean square error across all inhibition function fits was 0.0406, indicating very close fitting.

We performed a partial correlation analysis on the kinematic CRT coordination in the same way as RT correlations across effectors (Fig. 3D). Note that here we used CRTs rather than the interrupted movements as above, as it is a more direct measure. The head and arm showed the strongest relationship, with a partial correlation coefficient of  $\rho_{HA-E} = 0.752$  (0.521–0.873 individually) while the eye-head and eye-arm pairs showed weaker relationships, with coefficients of  $\rho_{EH-A} = 0.242$  (0.099–0.541) and  $\rho_{EA-H} = 0.331$  (–0.194–0.447), respectively. This pattern was different from the RT coordination, where eye-head correlations were strongest.

Next, we analyzed the time interval between the Go movement onset and the corrective movement onset (Fig. 9) separately for each participant and effector. We used the CRT-RT interval instead of the intermovement interval (end of first until beginning of next) because for arm and head movements the corrective movement could blend into the Go movement in interrupted movement trials (e.g., Fig. 2B) and thus there was no intermovement interval in those cases. For saccades (Fig. 9, top), we also included the histogram of Go saccade durations as a reference point. The minimal overlap between Go saccade durations and CRT-RT distributions is indicative of the successive nature of saccades, i.e., saccades were not interrupted once launched.

Figure 9 suggests that there was a continuum between rapid Go movement interruptions following the Stop signal (Fig. 2B)

and temporally segregated Go and corrective return movements (Fig. 2A). This was also apparent in the muscle EMG patterns for the head and arm. Figure 10 shows an example pattern across trials with corrective head movements. For rapid corrections after the Go movement onset, we observed a single antagonist muscle EMG burst that stopped the Go movement and drove the corrective movement back to center (e.g., see left trapezius/leftward target, trials 1–80; Fig. 10). For intermediate CRTs this single burst was stretched out in time (e.g., trials 80–130; Fig. 10), while long CRT trials show two distinct EMG bursts, one braking the Go movement and another burst initiating the corrective return movement (e.g., trials 130–155; Fig. 10). Thus RT and CRT motor commands showed different amounts of overlap depending on the corrective movement decision time rather than Go and corrective movements always being executed in series.

To understand corrective movement initiation, we evaluated a total of six different potential models for CRT distributions. CRT modeling focused only on the head and arm CRTs. Note that the EMG data for S3 and S7 showed poor signals for many trials; therefore, we fit CRT models to their kinematic data instead. The first model we fit (Fig. 11A) assumed that the corrective response is initiated when the decision signal of the Stop process reaches the threshold. This model showed a narrower and much faster CRT distribution than we observed behaviorally. In the second, related, model (Fig. 11B), we introduced an additional parameter capturing a potentially different (supposedly higher) threshold for the Stop process to initiate the corrective response, effectively delaying the mean latency of the CRT distribution. Note that this model is equivalent to a previously proposed model (Noorani and Carpenter 2015) in which the Stop process (they call this a Stop unit) was shifted in time, since a time shift or threshold change results in the same change of the underlying distribution; however, the resultant CRT distribution had a much longer tail than the data (similarly to the model in Fig. 11A). As such, these two models turned out to be overly simplistic and were discounted. Since the original Go/Stop signals were insufficient to describe CRTs, we introduced a separate second motor initiation process, “Go2,” specific to the corrective movement.

Using the Go2 process to describe CRTs, the third and fourth models, StopFinGo2 (Fig. 11C) and GoFinGo2 (Fig. 11D), capture return movement preparation as a separate motor decision signal (Go2) that starts after the Stop (Fig. 11C) or Go (Fig. 11D) signals reach the decision threshold. The CompressGo2 (Fig. 11E) model was developed to synthesize these two models by an intermediate model. In this model the Stop process is sped up once the Go process reaches threshold,

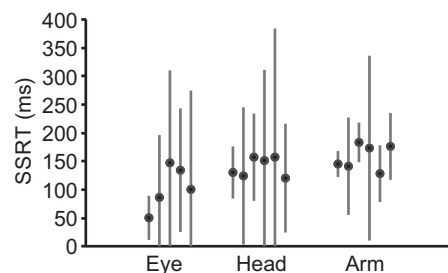


Fig. 6. SSRT estimates. Mean and SD of SSRTs were estimated from EMG data for all participants but S3 and S7, where kinematic data were used instead because of poor EMG quality. Bars are SE.

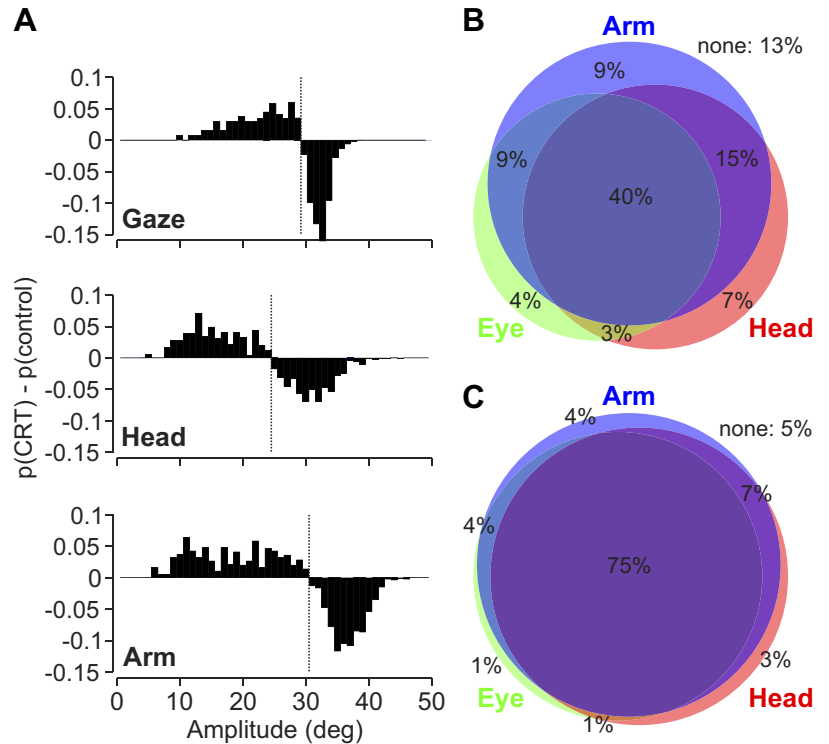


Fig. 7. Interrupted Go responses for eye, head, and arm. *A*: differential histograms of movement amplitudes for example participant 1. Difference between normalized CRT movement amplitude distribution  $p(\text{CRT})$  and control movement amplitude distribution  $p(\text{control})$  is shown. We used the zero crossing as a cutoff to determine interrupted movements (positive part of histogram). *B*: Venn diagram of proportion response interruptions for Stop trials where all effectors showed a Go response. *C*: same but for all Stop trials. Here, successfully inhibited responses were counted as interrupted Go processes.

analogous to removing a potential inhibitory action of the Go process onto the Stop process. This results in a temporal compression of the Stop process after the end of the Go1 process, increasing the rate of the Stop process. The Go2 process begins after this expedited completion of the Stop process. To model this, the residual time to threshold of the Stop process was reduced by a compression factor,  $C$ . The final model (Fig. 11*F*), Stop-StartGo2, represents a three-way race between the Go1 process, the Stop process, and the Go2 process, where the Go2 process begins at Stop signal onset and is therefore independent of the outcome of the race model. (Note: countermanding failure leads to an abortion of the Stop process in models in Fig. 11, *D* and *F*). This last model arose from the idea that, in uncertain environments, actions and corrective actions might be planned in parallel. Thus, as soon as the Stop signal is presented, the brain might, by default, plan a corrective action in case the Stop process fails. This model is very similar to the GO-GO+STOP model used to describe processes underlying double-step tasks (Camalier et al. 2007).

Figure 12 illustrates the overall iterative model fitting procedure (see METHODS) and model performance for kinematic arm movement data from participant S7. The RT fit (Fig. 12*A*)

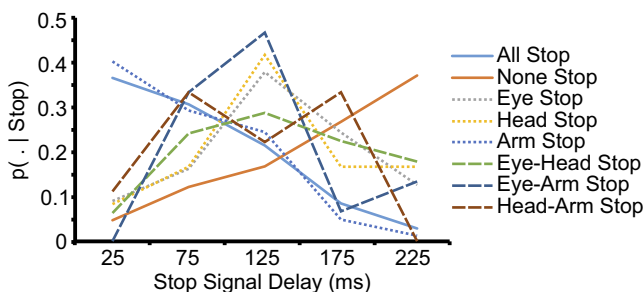


Fig. 8. Relative probability of effector inhibition combinations as a function of SSD. Proportions sum to 100% for each effector combination across SSDs.

was carried out first, and the result was then used to constrain the inhibition function fit (Fig. 12*B*). With these parameters being fixed, we fit the four different plausible CRT models to the data (Fig. 12*C*). In this example it can be readily observed that StopFinGo2 (Fig. 11*C*) and GoFinGo2 (Fig. 11*D*) did not capture the raw CRT data well. CompressGo2 (Fig. 11*E*) and StopStartGo2 (Fig. 11*F*) were only slightly different from one another, with CompressGo2 mainly capturing shorter CRTs better than StopStartGo2.

To determine which model performed best, we compared models according to three information criteria: BIC (Fig. 13*A*), AIC (Fig. 13*B*), and HQC (Fig. 13*C*). Information criterion measures were plotted separately for each participant and each kinematic/EMG-based measure and arranged by increasing BIC scores of the winning model, i.e., CompressGo2. Average and 95% CI values across all participants and modalities are also shown. In Fig. 13*D* we estimate the likelihood of the best model outperforming the others (see METHODS). This analysis shows that while the StopStartGo2 model (Fig. 11*F*) came close, the CompressGo2 model (Fig. 11*E*) consistently outperformed all other models.

We provide estimated parameters for the winning model (CompressGo2) in Table 4. Goodness of model fit was confirmed by Kolmogorov-Smirnov test, where we found no significant differences between model and data for all participants.  $P$  values were  $>0.9$  for all cases except for S7\_KH, where the  $P$  value was 0.654. For this specific fit, the model predicts a CRT distribution with a slight positive skew compared with the observed distribution; however, the source of this skew is unclear. Despite this, overall, model fits were highly significant.

To further analyze whether decision processes from different effectors were coupled, we compared model fit parameters across arm and head from Tables 2 and 4. If there was a

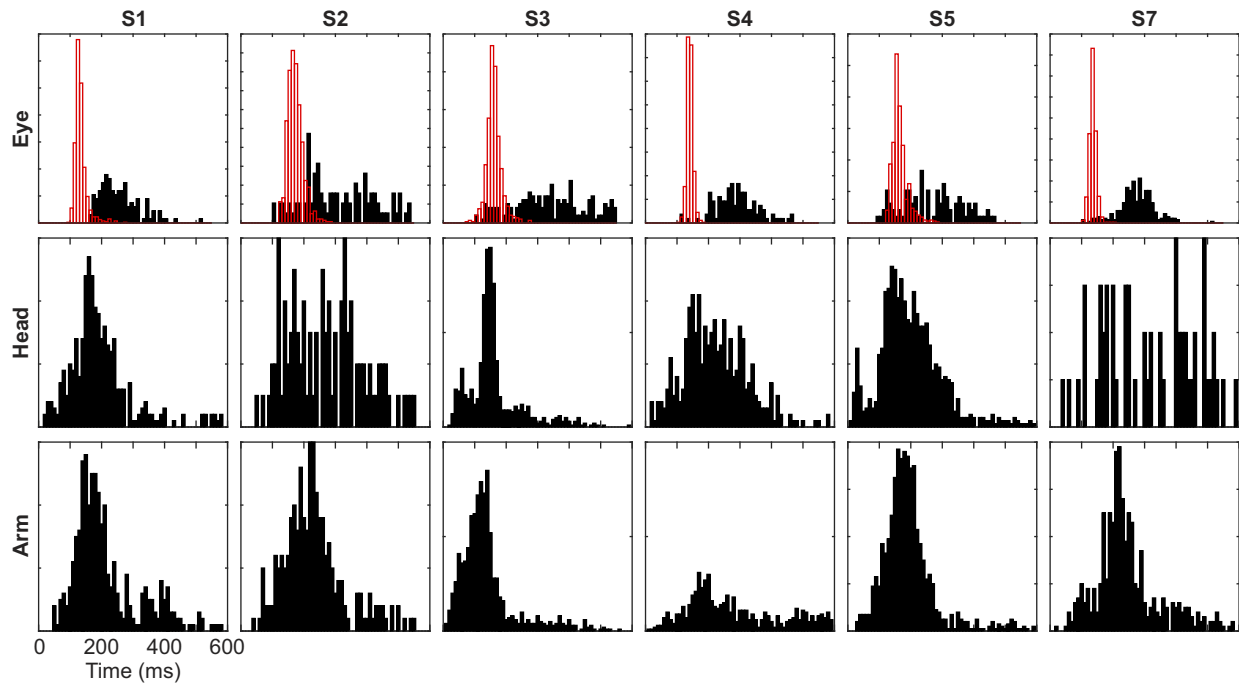


Fig. 9. Distribution of time intervals between Go movement onset (RT) and corrective movement onset (CRT). Black histograms show CRT-RT distributions for each participant and effector. Red histograms for eye movements also show Go saccade durations.

relationship between decision processes across effectors, then we expect the rate of rise of each decision process to be correlated across participants, i.e., a participant with a fast head decision process should also show a fast hand decision process. This analysis to test this hypothesis is shown in Fig. 14. While individual correlations of RT, CRT, and SSRT only proved to

be significant for CRT ( $P = 0.0011$ ), pooling across all processes resulted in a highly significant relationship. On average, RT processes took the longest (smallest rates), followed by SSRT and CRT, with the variance across participants increasing from RT to SSRT to CRT. Also interestingly, while for RT and SSRT the head was faster than the arm (as reflected

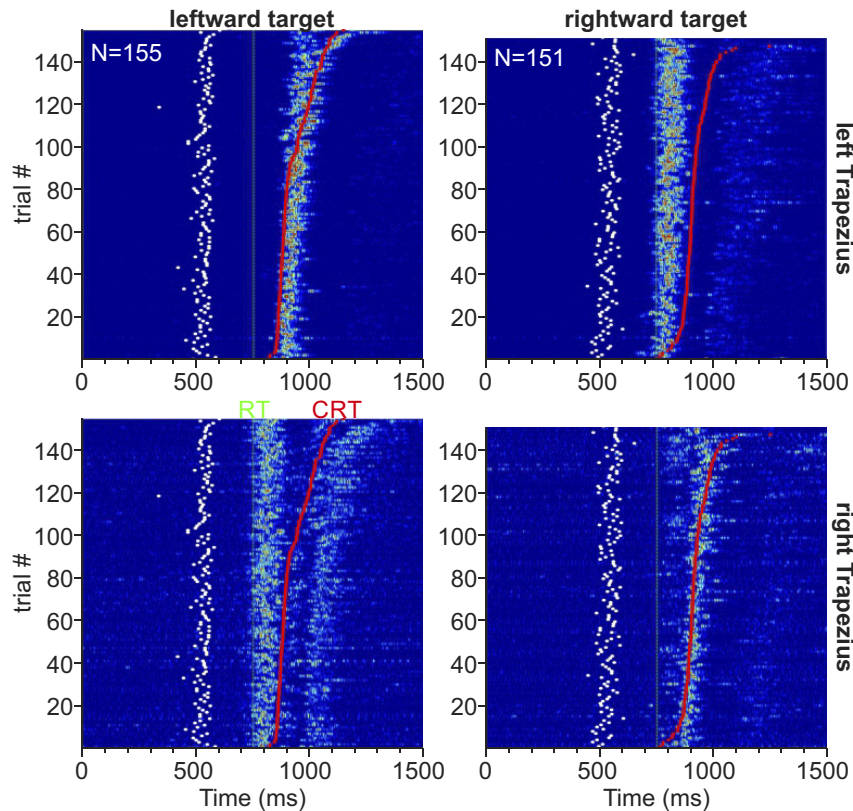


Fig. 10. Example head EMG activations [left (top) and right (bottom) trapezius muscle] from S5 during stop trials containing erroneous leftward (left) and rightward (right) movements. Data are aligned to the movement initiation (RT, green markers) based on EMG. Red markers depict corrective movement initiation (CRT) based on EMG. White markers indicate target onset times.

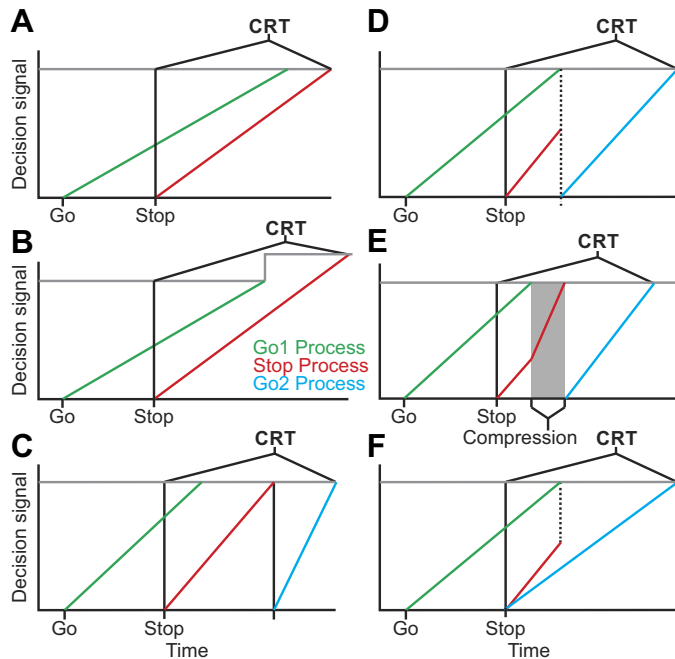


Fig. 11. Tested model alternatives. A: StopCRT. B: StopCRTth. C: StopFinGo2. D: GoFinGo2. E: CompressGo2. F: StopStartGo2. See text for details.

in higher head vs. arm process rates), this was the opposite for CRTs, where the arm was faster. We also looked for relationships between RT, SSRT, and CRT rates within each effector but did not find any significant correlations, indicating independence of those processes. Overall, this analysis shows that arm and head processes were at least partially correlated but displayed a significant amount of individual variability.

**DISCUSSION**

The main aim of this study was to investigate response and corrective movement initiation during a combined gaze shift

and pointing countermanding task. We found that overall response and corrective movement initiation times were well correlated between the different effectors, with some differences in the degree of correlation between effectors according to the type of response (RT vs. CRT). To gain insight into the underlying decision processes involved in corrective movement initiation, we tested several extended LATER race models and found that the best-fitting model was one that presumed that the corrective movement initiation was triggered after an accelerated (failed) inhibition process was completed. Taken together these results suggest that corrective movement initiation is dependent on dynamic inhibition processes and that the same decision processes may trigger multiple effectors during coordinated movement tasks for both responses and corrective movements.

*Response Times Across Different Effectors*

On Go trials, the RTs of the eyes, head, and arm demonstrated mutual coordination between effectors, i.e., when the head RT was quick, the eye and arm RT tended to also be quick, within their respective RT distributions. When comparing RTs for each effector to each of the other two we found that the strongest relationship was between the eyes and the head (partial correlation of 0.724) and found lesser but significant correlations between the eye and the arm (partial correlation of 0.303) and between the head and the arm (partial correlation of 0.306). Our results are consistent with other studies on eye-head-arm motor coordination (Biguer et al. 1982; Gielen et al. 1984) and support evidence for a shared initiation processes across effectors for eye-head (Freedman 2008; Khan et al. 2009) and eye-arm (Fischer and Rogal 1986; Gopal and Murthy 2015; Gribble et al. 2002; Stuphorn et al. 2000; Suzuki et al. 2008) movements.

The high correlation between RTs of the eye and the head is not surprising considering the close coupling between the eye and head during gaze shifts. Indeed, it is generally accepted that there is a major common gaze drive for both head and

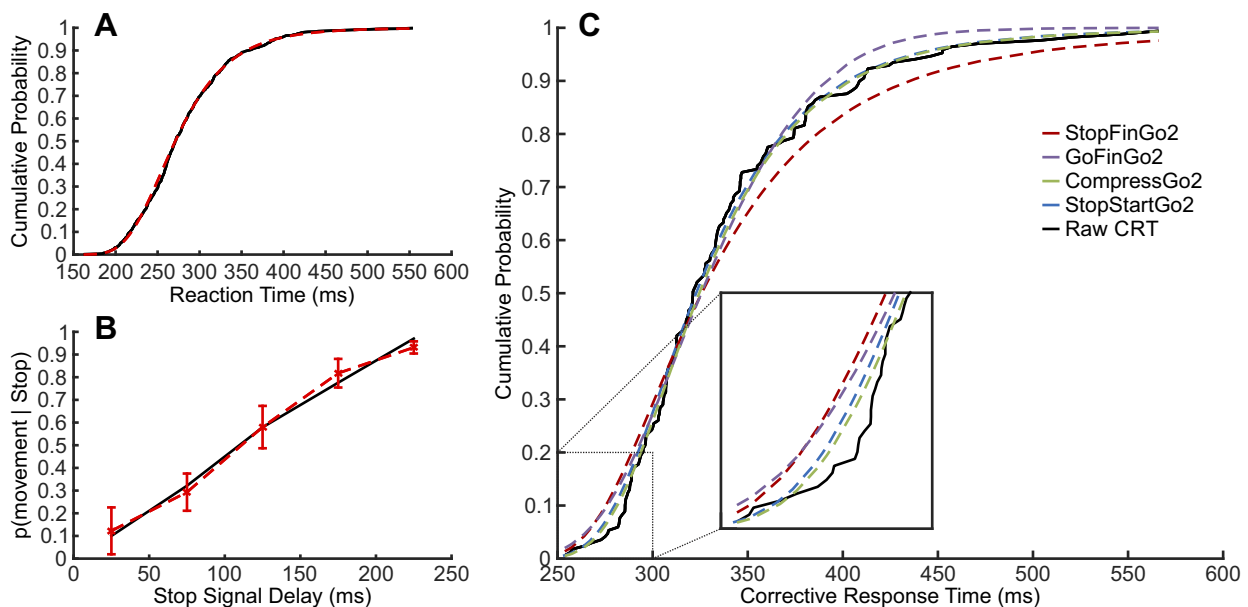


Fig. 12. A and B: model fitting of S7 kinematic arm data for reaction time with raw data (black) and fitted distribution (red) (A) and inhibition function where the proportion of inhibition failure (stop-failure) increased with increasing Stop signal delay [B; bars denote confidence intervals of the model (red)]. C: raw CRTs and 4 different model fits.

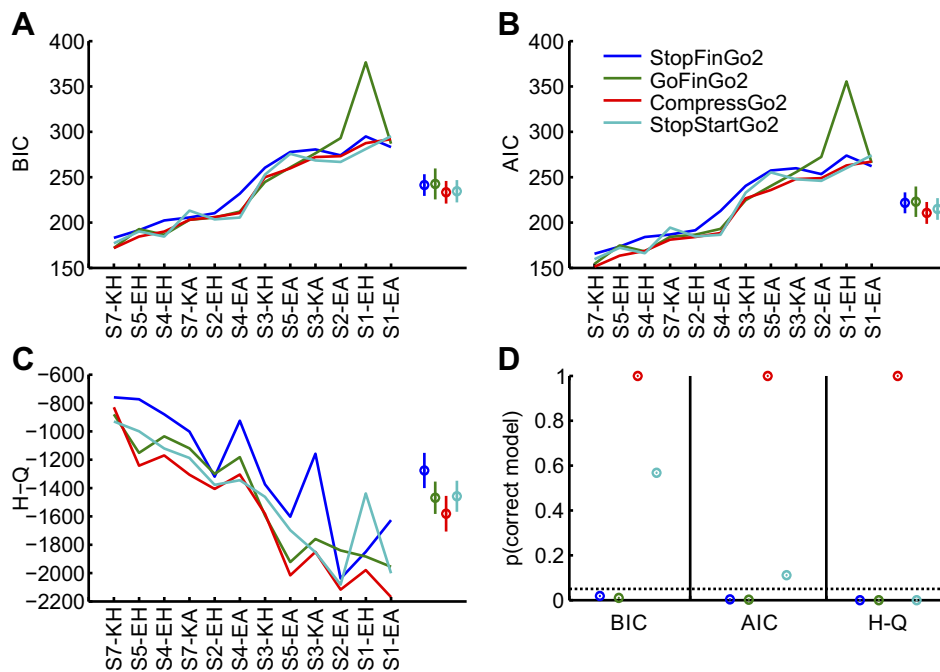


Fig. 13. *A*: model fit comparison with Bayesian information criterion (BIC). Mean  $\pm$  SD of model scores are  $241.3 \pm 41.2$  (StopFinGo2),  $242.5 \pm 59.1$  (GoFinGo2),  $233.4 \pm 43.3$  (CompressGo2), and  $234.5 \pm 42.7$  (StopStartGo2), as shown by the colored circles with SE bars. *B*: model fit comparison with Akaike information criterion (AIC). Mean  $\pm$  SD of model scores are  $221.8 \pm 39.9$  (StopFinGo2),  $223.0 \pm 58.0$  (GoFinGo2),  $210.6 \pm 41.8$  (CompressGo2), and  $215.0 \pm 41.5$  (StopStartGo2). *C*: model fit comparison with Hannan-Quinn information criterion (H-Q). Mean  $\pm$  SD of model scores are  $-1,276 \pm 431$  (StopFinGo2),  $-1,469 \pm 396$  (GoFinGo2),  $-1,581 \pm 435$  (CompressGo2), and  $-1,458 \pm 380$  (StopStartGo2). Absolute numbers are arbitrary, but the smaller the number, the better the model fits the behavior. *D*: comparative likelihoods of correct model for each information criterion separately.

saccade movements (Bizzi et al. 1972; Daye et al. 2014; Freedman and Sparks 1997; Haji-Abolhassani et al. 2016; Hanes and McCollum 2006; Monteon et al. 2005; Oommen et al. 2004; Oommen and Stahl 2005; Zangemeister and Stark 1982). However, there also is evidence of a separate pathway for the initiation of head movements during combined eye-head gaze shifts (Bizzi et al. 1972; Hanes and McCollum 2006; Oommen and Stahl 2005; Zangemeister and Stark 1982). Thus the high but not perfect correlation between the head and the eye RTs may reflect decision processes that descend through both shared and independent pathways for the head and the eye. An alternate explanation may be that the shared gaze drive is used but eye movement initiation times are shuffled because of the omnipause neuron gating system, whereas head movements are not (Gandhi and Sparks 2007).

While arm RTs were significantly correlated with the other effectors, the correlation was much weaker. These differences indicate that the arm, while sharing some coordinated processing with the eye and head, retains a larger degree of independence in terms of its stochastic initiation process. Within the literature there have been mixed results in terms of the correlation between RTs of the eye and the arm, ranging from very low to very high correlations (Frens and Erkelens 1991; Gopal and Murthy 2015; Herman et al. 1981; Prablanc et al. 1979; Sailer et al. 2000; Vercher et al. 1994). Similarly, recent studies have proposed contrasting models, either relatively independent but mutually exciting integrators (Dean et al. 2011) or alternatively coordinated accumulators to drive the coordinated movement (Gopal and Murthy 2015). However, it has been recently suggested that task context could determine the amount of linkage between the two processes (Jana et al. 2017), an important factor that may explain these different findings.

#### Response Inhibition Across Effectors

During successful Stop trials, we found different patterns of inhibition across effectors. As outlined in Table 3, the most common case was the successful inhibition of all three effec-

tors together (73%). The remainder of the trials (27%) consisted of some combination of successful inhibition and movement response, with the second most common combination being the coupled inhibition of the eye and the head but not the arm (11%) followed by the eye only but not the arm or head (7%) and the arm alone (5%). Finally, there were very few trials (<1% each) where the eye and arm but not the head, the head and arm but not the eye, or the head alone was inhibited. These combinations indicate that there is likely a single or at least very closely linked inhibition processes for the three effectors together given that the vast majority of successful Stop trials were those where all three effectors were inhibited together. If each effector's race signal was purely independent, we would expect to see a much higher proportion of other inhibition combinations, e.g., head-only inhibition. Furthermore, these results indicate a strong coupling of inhibition between the eye and head. Given the strong partial correlation of eye and head RTs, the coupling of eye and head inhibition is unsurprising. We speculate that the inhibition process of the eye may be expediting the inhibition process of the head, likely mediated through the common gaze drive mentioned above. These findings are similar to previous studies, which also found a linkage between inhibition processes for saccades and head movements (Corneil and Elsley 2005).

However, we also found some evidence for independence of inhibition of the eye only. First, the highest percentage of single effector inhibition was that of the eye (7%). Second, the lowest and fastest inhibition rates for eye movements also suggest that the Stop process for the eye is particularly efficient (relative to the eye Go process), in comparison to the head and arm.

Finally, the relative independence of the arm from the eye and the head is consistent with the lower partial correlations of RTs of the arm with the other effectors, indicating a larger independence of decision processes between the arm and the other two effectors. However, it should be noted that in the majority of successful Stop trials the arm movement was

Table 4. Summary of fitted CRT parameters for CompressGo2 model

		Parameter, s <sup>-1</sup>	95% CI	K-S Test P Value
S1	EMG head	C	0.652 [0.620, 0.684]	0.929
		$\mu_{\text{rate}}$	18.866 [17.621, 20.112]	
		$\sigma_{\text{rate}}$	5.452 [4.629, 6.274]	
	EMG arm	C	0.6695 [0.657, 0.682]	0.997
		$\mu_{\text{rate}}$	20.144 [19.605, 20.683]	
		$\sigma_{\text{rate}}$	8.401 [7.841, 8.962]	
S2	EMG head	C	0.357 [0.228, 0.487]	0.968
		$\mu_{\text{rate}}$	5.966 [5.749, 6.184]	
		$\sigma_{\text{rate}}$	1.595 [1.540, 1.650]	
	EMG arm	C	0.744 [0.708, 0.779]	0.999
		$\mu_{\text{rate}}$	10.093 [9.741, 10.445]	
		$\sigma_{\text{rate}}$	2.173 [2.026, 2.321]	
S3	KIN head	C	0.079 [-1.354, 1.513]	0.967
		$\mu_{\text{rate}}$	2.935 [2.161, 3.689]	
		$\sigma_{\text{rate}}$	0.556 [0.457, 0.655]	
	KIN arm	C	1.0000 [4.958, 5.037]	0.912
		$\mu_{\text{rate}}$	4.997 [1.356, 1.407]	
		$\sigma_{\text{rate}}$	1.381 [1.356, 1.407]	
S4	EMG head	C	0.298 [0.205, 0.392]	0.984
		$\mu_{\text{rate}}$	7.532 [7.288, 7.775]	
		$\sigma_{\text{rate}}$	0.100 [-1.800, 2.00]	
	EMG arm	C	0.145 [0.104, 0.185]	0.992
		$\mu_{\text{rate}}$	8.951 [8.670, 9.233]	
		$\sigma_{\text{rate}}$	0.040 [-0.492, 0.572]	
S5	EMG head	C	0.0017 [0.0013, 0.0021]	0.944
		$\mu_{\text{rate}}$	6.249 [6.193, 6.306]	
		$\sigma_{\text{rate}}$	1.589 [1.447, 1.731]	
	EMG arm	C	0.199 [-0.289, 0.686]	0.999
		$\mu_{\text{rate}}$	6.199 [5.720, 6.677]	
		$\sigma_{\text{rate}}$	2.009 [1.795, 2.223]	
S7	KIN head	C	0.507 [0.319, 0.695]	0.654
		$\mu_{\text{rate}}$	4.112 [3.931, 4.292]	
		$\sigma_{\text{rate}}$	0.132 [-9.91, 10.214]	
	KIN arm	C	0.765 [0.660, 0.870]	0.965
		$\mu_{\text{rate}}$	6.161 [5.938, 6.384]	
		$\sigma_{\text{rate}}$	0.107 [0.027, 0.187]	

Parameters  $\mu_{\text{rate}}$  and  $\sigma_{\text{rate}}$  describe the normal rate distribution governing the Go2 LATER process. Parameter C defines the compression ratio applied to the residual Stop process after Go1 reaches threshold.

inhibited along with the eye and the head. Consistent with these findings, Leung and Cai (2007) showed that the ventrolateral prefrontal cortex may play a role in inhibition processes of both oculomotor and hand motor systems. This is also consistent with the notion of a global motor mechanism that exerts inhibition on all ongoing motor plans, regardless of effector (Pouget et al. 2017), which may be implemented via broad inhibition from the basal ganglia to the cortex (Aron et al. 2003; Schmidt et al. 2013). However, other studies have shown no relationship in inhibition processes between saccades and hand movements, suggesting that independent hand control may be preferred over coupling in coordinated movements involving multiple effectors (Boucher et al. 2007). Taken together, it appears that the inhibition processes for the three effectors are tightly linked but with some degree of independence between them (more so with the arm than between the eye and hand).

### Corrective Response Initiation Compared Across Effectors

We compared corrective response initiation across effectors in two ways. First, we compared amplitudes of failed Stop and Go trials as an indicator of interrupted movements. Comparing across effectors, the pattern of interruptions between the three effectors (Fig. 7) was very similar to the patterns observed for inhibition (Stop trial outcomes) across the effectors (Table 3). We observed that, in the majority of trials, all three effectors demonstrated reduced amplitudes indicative of response interruption. However, there were some independent reductions in amplitude for arm movements compared with head or eye movements, which almost always occurred together. This is consistent with a predominantly common process driving inhibition across effectors.

We also measured corrective response initiation directly through CRTs. For arm and head, these were calculated using responses in the antagonist muscles; for eye movements, kinematics were used (return eye movement latency). In contrast to the RTs and inhibition, we found a stronger relationship between the head and arm effectors for corrective response initiation compared with the eye. We speculate that this is due to the slower movements of the head and arm, where in-flight modifications are more likely, compared with the faster movements of saccades, which have less time available for modification. However, the eye CRTs nevertheless showed mild correlations with the head and arm CRTs, indicating that the eye corrective response still shares a temporal relationship with the head and arm as also demonstrated through the interrupted movement analysis.

### CRT Modeling

To gain insight into the decision processes involving corrective movement initiation during failed Stop trials, we evaluated different models and determined how well they fit our observed CRT distributions. In the first two models, we assumed that the corrective movement was initiated when the decision signal for the Stop process reached the same or a slightly higher threshold (Fig. 11, A and B), analogous to the model proposed by Noorani and Carpenter (2015); however, they failed to match the behavioral findings well and were overly simplistic. This prompted the development of models

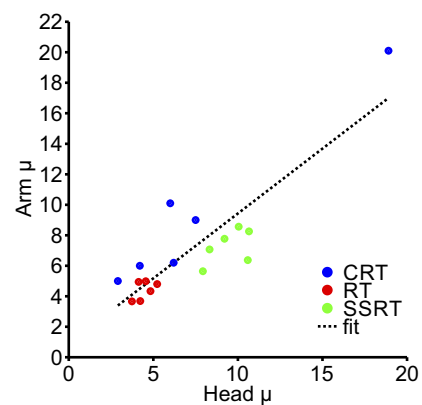


Fig. 14. Relationship between best fit model rates  $\mu$  (inverse of RT) across effectors. CRT, RT, and SSRT mean LATER rates across participants. Linear fit between arm and head processes across all rates  $\mu$  was highly significant ( $y = 0.919 + 0.8511x$ ,  $P < 0.001$ ), even when excluding the large CRT outlier.

that included a second motor initiation process, Go2. In the next two models, the second Go process was initiated either when the Stop process (StopFinGo2; Fig. 11C) or the Go process (GoFinGo2; Fig. 11D) reached threshold. In the third model, the second Go process was initiated after an accelerated Stop process once the Go process reached threshold (CompressGo2; Fig. 11E). Finally, we also evaluated a model where the second Go process was initiated at the same time as the Stop process and was independent of the outcome of the race model (StopStartGo2; Fig. 11F).

In the evaluation of such probabilistic models, there is no single exact method for selecting the “best” model. We chose to rank our models according to three different information criteria, each with different strengths, weaknesses, and popularity of usage. Our strategy was to look for consistency of performance in a model across criteria. All criteria demonstrated identical relative rankings of models for each case. Our rankings suggest the CompressGo2 model as the strongest model for CRTs under our extended countermanding paradigm. The StopFinGo2 model demonstrated the worst quality of the four models ranked. Interestingly, the StopStartGo2 proved to be a relatively strong model for some cases and a much weaker model in others.

Under the CompressGo2 model, the initiation of the Go2 process is dependent on the progress of the Stop process, i.e., the Go2 process must “wait” for the expedited Stop process to complete. Considering the wide range of the compression factors (<1% to 100%, see parameter C in Table 4) in our results, the degree of such dependence seems to be highly subject—and effector—specific. With respect to the complexity of our motor task, this compression factor may be capturing the influence of a number of factors: coordination, top-down strategy, or residual inhibition of the Stop process after the race has been decided. The presence of this compression factor in the model suggests that conflict in decision making, particularly when making a mistake, has an effect in terms of neural processing on subsequent decisions.

The Go2GoFin model closely resembles the model proposed by Noorani and Carpenter (2014) to describe CRTs in the antisaccade task. In their task, participants were asked to generate a saccade in the opposite direction of a visual target, and they investigated the RTs of corrective movements that took place after antisaccade errors (whereby prosaccades are generated, followed by saccades in the correct antidirection). These authors modeled the antisaccade task as three LATER races involving two identical initiation processes (prosaccade and antisaccade) and a Stop process that suppresses the erroneous response (prosaccade) for each trial; upon failure to suppress the prosaccade, the antisaccade unit is restarted. This model is analogous to our GoFinGo2 model, except that we do not assume the corrective response is governed by the same LATER process as the initial motor response, i.e., the process’s parameters can be different. In contrast to their findings, we found this model to fit the behavioral CRT data in our task less well than the CompressGo2 model. It is possible that these more parsimonious models, StopStartGo2 and GoFinGo2, may explain CRTs under specific cognitive conditions, for example, in more rigidly structured countermanding experiments with single effector tasks such as the task used by Noorani and Carpenter (2014).

The StopStartGo2 model, our second strongest model, is very similar to that used to model saccade behavior during double-step and step search tasks (Camalier et al. 2007). They found that their version of the StopStartGo2 model (GO-GO+STOP model) best fit the pattern and timing of compensated vs. noncompensated eye movements to variably timed jumps in target position. Interestingly, they also showed evidence of interrupted saccades with initial saccades with shorter amplitudes (labeled partial compensated) as used in our interrupted movement analysis (Fig. 7). However, Camalier et al. (2007) did not consider the possibility of an accelerated finish of the Stop signal after erroneous Go initiation, as in our best-performing model (CompressGo2). It would be interesting to evaluate the CompressGo2 model against the Camalier et al. (2007) paradigm to verify whether accelerated termination of competing decision processes might also explain their data.

Finally, while we utilized the stop-signal paradigm as our task (Logan and Cowan 1984), response initiation, inhibition, and error correction can also be driven by different task requirements such as during the antisaccade (Noorani and Carpenter 2013), double-step (Becker and Jürgens 1979; Camalier et al. 2007; Georgopoulos et al. 1983), or color oddity (McPeck and Keller 2002; Moher and Song 2013; Noorani et al. 2011; Song 2017) tasks as well as internal signals such as individual goals or previous errors (Song 2017). Whether internal or external, evidence suggests that the underlying mechanisms for coordination across multiple effector planning are similar (Pouget et al. 2017).

### Conclusions

In this study, we evaluated the performance of an eye-head-arm motor task under a countermanding paradigm. Motor initiation was shown to be correlated between all effectors, with the strongest relationship between the eye and head. Patterns of partial inhibition largely favor coupling between all three effectors, as did the pattern of interrupted and corrective movements. We introduced new models to explain the RTs of corrective responses in the countermanding task; the prevailing model relies on a second motor initiation process that begins after the residual Stop process reaches threshold in an expedited fashion. We thus conclude that the processing of corrective actions is influenced by previous erroneous actions.

### GRANTS

G. Blohm is supported by Natural Sciences and Engineering Research Council of Canada (NSERC), Ontario Research Fund, and Canada Foundation for Innovation grants. A. Z. Khan holds a Canada Research Chair and a NSERC grant.

### DISCLOSURES

No conflicts of interest, financial or otherwise, are declared by the authors.

### AUTHOR CONTRIBUTIONS

G.T. and G.B. conceived and designed research; G.T. performed experiments; G.T., A.Z.K., and G.B. analyzed data; G.T., A.Z.K., and G.B. interpreted results of experiments; G.T. and G.B. prepared figures; G.T. drafted manuscript; A.Z.K. and G.B. edited and revised manuscript; G.T., A.Z.K., and G.B. approved final version of manuscript.

## REFERENCES

- Aron AR.** The neural basis of inhibition in cognitive control. *Neuroscientist* 13: 214–228, 2007. doi:10.1177/1073858407299288.
- Aron AR, Schlaghecken F, Fletcher PC, Bullmore ET, Eimer M, Barker R, Sahakian BJ, Robbins TW.** Inhibition of subliminally primed responses is mediated by the caudate and thalamus: evidence from functional MRI and Huntington's disease. *Brain* 126: 713–723, 2003.
- Becker W, Jürgens R.** An analysis of the saccadic system by means of double step stimuli. *Vision Res* 19: 967–983, 1979. doi:10.1016/0042-6989(79)90222-0.
- Bekkering H, Pratt J, Abrams RA.** The gap effect for eye and hand movements. *Percept Psychophys* 58: 628–635, 1996. doi:10.3758/BF03213095.
- Beuk J, Beninger RJ, Paré M.** Investigating a race model account of executive control in rats with the countermanding paradigm. *Neuroscience* 263: 96–110, 2014. doi:10.1016/j.neuroscience.2014.01.014.
- Biguer B, Jeannerod M, Prablanc C.** The coordination of eye, head, and arm movements during reaching at a single visual target. *Exp Brain Res* 46: 301–304, 1982. doi:10.1007/BF00237188.
- Bizzi E, Kalil R, Morasso P, Tagliacozzo V.** Central programming and peripheral feedback during eye-head coordination in monkeys. *Bibl Ophthalmol* 82: 220, 1972.
- Boucher L, Stuphorn V, Logan GD, Schall JD, Palmeri TJ.** Stopping eye and hand movements: are the processes independent? *Percept Psychophys* 69: 785–801, 2007. doi:10.3758/BF03193779.
- Burnham KP, Anderson DR.** *Model Selection and Multimodel Inference: a Practical Information-Theoretic Approach*. New York: Springer Science & Business Media, 2003.
- Camalier CR, Gotler A, Murthy A, Thompson KG, Logan GD, Palmeri TJ, Schall JD.** Dynamics of saccade target selection: race model analysis of double step and search step saccade production in human and macaque. *Vision Res* 47: 2187–2211, 2007. doi:10.1016/j.visres.2007.04.021.
- Carey DP.** Eye-hand coordination: eye to hand or hand to eye? *Curr Biol* 10: R416–R419, 2000. doi:10.1016/S0960-9822(00)00508-X.
- Carpenter R.** Oculomotor procrastination. In: *Eye Movements. Cognition and Visual Perception*, edited by Fisher DF, Monty RA, Senders JW. Hillsdale, NJ: Erlbaum, 1981, p. 237–246.
- Chambers CD, Garavan H, Bellgrove MA.** Insights into the neural basis of response inhibition from cognitive and clinical neuroscience. *Neurosci Biobehav Rev* 33: 631–646, 2009. doi:10.1016/j.neubiorev.2008.08.016.
- Chou IH, Sommer MA, Schiller PH.** Express averaging saccades in monkeys. *Vision Res* 39: 4200–4216, 1999. doi:10.1016/S0042-6989(99)00133-9.
- Coe BC, Munoz DP.** Mechanisms of saccade suppression revealed in the anti-saccade task. *Philos Trans R Soc Lond B Biol Sci* 372: 20160192, 2017. doi:10.1098/rstb.2016.0192.
- Corneil BD, Elsley JK.** Countermanding eye-head gaze shifts in humans: marching orders are delivered to the head first. *J Neurophysiol* 94: 883–895, 2005. doi:10.1152/jn.01171.2004.
- Corneil BD, Munoz DP.** Human eye-head gaze shifts in a distractor task. II. Reduced threshold for initiation of early head movements. *J Neurophysiol* 82: 1406–1421, 1999. doi:10.1152/jn.1999.82.3.1406.
- Corneil BD, Olivier E, Munoz DP.** Neck muscle responses to stimulation of monkey superior colliculus. I. Topography and manipulation of stimulation parameters. *J Neurophysiol* 88: 1980–1999, 2002. doi:10.1152/jn.2002.88.4.1980.
- Cutsuridis V.** Behavioural and computational varieties of response inhibition in eye movements. *Philos Trans R Soc Lond B Biol Sci* 372: 20160196, 2017. doi:10.1098/rstb.2016.0196.
- Daye PM, Optican LM, Blohm G, Lefèvre P.** Hierarchical control of two-dimensional gaze saccades. *J Comput Neurosci* 36: 355–382, 2014. doi:10.1007/s10827-013-0477-1.
- Dean HL, Martí D, Tsui E, Rinzal J, Pesaran B.** Reaction time correlations during eye-hand coordination: behavior and modeling. *J Neurosci* 31: 2399–2412, 2011. doi:10.1523/JNEUROSCI.4591-10.2011.
- Domagalik A, Beldzik E, Fafrowicz M, Oginska H, Marek T.** Neural networks related to pro-saccades and anti-saccades revealed by independent component analysis. *Neuroimage* 62: 1325–1333, 2012. doi:10.1016/j.neuroimage.2012.06.006.
- Fischer B, Rogal L.** Eye-hand-coordination in man: a reaction time study. *Biol Cybern* 55: 253–261, 1986. doi:10.1007/BF00355600.
- Fisk JD, Goodale MA.** The organization of eye and limb movements during unrestricted reaching to targets in contralateral and ipsilateral visual space. *Exp Brain Res* 60: 159–178, 1985. doi:10.1007/BF00237028.
- Freedman EG.** Coordination of the eyes and head during visual orienting. *Exp Brain Res* 190: 369–387, 2008. doi:10.1007/s00221-008-1504-8.
- Freedman EG, Sparks DL.** Activity of cells in the deeper layers of the superior colliculus of the rhesus monkey: evidence for a gaze displacement command. *J Neurophysiol* 78: 1669–1690, 1997. doi:10.1152/jn.1997.78.3.1669.
- Freedman EG, Sparks DL.** Coordination of the eyes and head: movement kinematics. *Exp Brain Res* 131: 22–32, 2000. doi:10.1007/s002219900296.
- Frens MA, Erkelens CJ.** Coordination of hand movements and saccades: evidence for a common and a separate pathway. *Exp Brain Res* 85: 682–690, 1991. doi:10.1007/BF00231754.
- Gandhi NJ, Sparks DL.** Dissociation of eye and head components of gaze shifts by stimulation of the omnipause neuron region. *J Neurophysiol* 98: 360–373, 2007. doi:10.1152/jn.00252.2007.
- Georgopoulos AP, Kalaska JF, Caminiti R, Massey JT.** Interruption of motor cortical discharge subserving aimed arm movements. *Exp Brain Res* 49: 327–340, 1983. doi:10.1007/BF00238775.
- Gielen CC, van den Heuvel PJ, van Gisbergen JA.** Coordination of fast eye and arm movements in a tracking task. *Exp Brain Res* 56: 154–161, 1984. doi:10.1007/BF00237452.
- Goonetilleke SC, Katz L, Wood DK, Gu C, Huk AC, Corneil BD.** Cross-species comparison of anticipatory and stimulus-driven neck muscle activity well before saccadic gaze shifts in humans and nonhuman primates. *J Neurophysiol* 114: 902–913, 2015. doi:10.1152/jn.00230.2015.
- Gopal A, Murthy A.** Eye-hand coordination during a double-step task: evidence for a common stochastic accumulator. *J Neurophysiol* 114: 1438–1454, 2015. doi:10.1152/jn.00276.2015.
- Gribble PL, Everling S, Ford K, Mattar A.** Hand-eye coordination for rapid pointing movements. Arm movement direction and distance are specified prior to saccade onset. *Exp Brain Res* 145: 372–382, 2002. doi:10.1007/s00221-002-1122-9.
- Groman SM, James AS, Jentsch JD.** Poor response inhibition: at the nexus between substance abuse and attention deficit/hyperactivity disorder. *Neurosci Biobehav Rev* 33: 690–698, 2009. doi:10.1016/j.neubiorev.2008.08.008.
- Guitton D, Munoz DP, Galiana HL.** Gaze control in the cat: studies and modeling of the coupling between orienting eye and head movements in different behavioral tasks. *J Neurophysiol* 64: 509–531, 1990. doi:10.1152/jn.1990.64.2.509.
- Guitton D, Volle M.** Gaze control in humans: eye-head coordination during orienting movements to targets within and beyond the oculomotor range. *J Neurophysiol* 58: 427–459, 1987. doi:10.1152/jn.1987.58.3.427.
- Haji-Abolhassani I, Guitton D, Galiana HL.** Modeling eye-head gaze shifts in multiple contexts without motor planning. *J Neurophysiol* 116: 1956–1985, 2016. doi:10.1152/jn.00605.2015.
- Hakvoort Schwerdtfeger RM, Alahyane N, Brien DC, Coe BC, Stroman PW, Munoz DP.** Preparatory neural networks are impaired in adults with attention-deficit/hyperactivity disorder during the antisaccade task. *Neuroimage Clin* 2: 63–78, 2012. doi:10.1016/j.nicl.2012.10.006.
- Hanes DA, McCollum G.** Variables contributing to the coordination of rapid eye/head gaze shifts. *Biol Cybern* 94: 300–324, 2006. doi:10.1007/s00422-006-0049-9.
- Hanes DP, Carpenter RH.** Countermanding saccades in humans. *Vision Res* 39: 2777–2791, 1999. doi:10.1016/S0042-6989(99)00011-5.
- Hanes DP, Patterson WF 2nd, Schall JD.** Role of frontal eye fields in countermanding saccades: visual, movement, and fixation activity. *J Neurophysiol* 79: 817–834, 1998. doi:10.1152/jn.1998.79.2.817.
- Hanes DP, Schall JD.** Countermanding saccades in macaque. *Vis Neurosci* 12: 929–937, 1995. doi:10.1017/S095252380009482.
- Herman R, Herman R, Maulucci R.** Visually triggered eye-arm movements in man. *Exp Brain Res* 42: 392–398, 1981.
- Jana S, Gopal A, Murthy A.** Evidence of common and separate eye and hand accumulators underlying flexible eye-hand coordination. *J Neurophysiol* 117: 348–364, 2017. doi:10.1152/jn.00688.2016.
- Jantz JJ, Watanabe M, Everling S, Munoz DP.** Threshold mechanism for saccade initiation in frontal eye field and superior colliculus. *J Neurophysiol* 109: 2767–2780, 2013. doi:10.1152/jn.00611.2012.
- Jeannerod M.** *The Neural and Behavioural Organization of Goal-Directed Movements*. Oxford, UK: Clarendon, 1988.
- Khan AZ, Blohm G, McPeck RM, Lefèvre P.** Differential influence of attention on gaze and head movements. *J Neurophysiol* 101: 198–206, 2009. doi:10.1152/jn.90815.2008.

- Khan AZ, Blohm G, Pisella L, Munoz DP.** Saccade execution suppresses discrimination at distractor locations rather than enhancing the saccade goal location. *Eur J Neurosci* 41: 1624–1634, 2015. doi:10.1111/ejn.12923.
- Leung HC, Cai W.** Common and differential ventrolateral prefrontal activity during inhibition of hand and eye movements. *J Neurosci* 27: 9893–9900, 2007. doi:10.1523/JNEUROSCI.2837-07.2007.
- Logan GD, Cowan WB.** On the ability to inhibit thought and action: a theory of an act of control. *Psychol Rev* 91: 295–327, 1984. doi:10.1037/0033-295X.91.3.295.
- Mattia M, Spadacenta S, Pavone L, Quarato P, Esposito V, Sparano A, Sebastiano F, Di Gennaro G, Morace R, Cantore G, Mirabella G.** Stop-event-related potentials from intracranial electrodes reveal a key role of premotor and motor cortices in stopping ongoing movements. *Front Neuroeng* 5: 12, 2012. doi:10.3389/fneng.2012.00012.
- McPeck RM, Han JH, Keller EL.** Competition between saccade goals in the superior colliculus produces saccade curvature. *J Neurophysiol* 89: 2577–2590, 2003. doi:10.1152/jn.00657.2002.
- McPeck RM, Keller EL.** Short-term priming, concurrent processing, and saccade curvature during a target selection task in the monkey. *Vision Res* 41: 785–800, 2001. doi:10.1016/S0042-6989(00)00287-X.
- McPeck RM, Keller EL.** Saccade target selection in the superior colliculus during a visual search task. *J Neurophysiol* 88: 2019–2034, 2002. doi:10.1152/jn.2002.88.4.2019.
- Minken AW, Van Opstal AJ, Van Gisbergen JA.** Three-dimensional analysis of strongly curved saccades elicited by double-step stimuli. *Exp Brain Res* 93: 521–533, 1993. doi:10.1007/BF00229367.
- Moher J, Song JH.** Context-dependent sequential effects of target selection for action. *J Vis* 13: 10, 2013. doi:10.1167/13.8.10.
- Monteon JA, Martinez-Trujillo JC, Wang H, Crawford JD.** Cross-coupled adaptation of eye and head position commands in the primate gaze control system. *Neuroreport* 16: 1189–1192, 2005. doi:10.1097/00001756-200508010-00011.
- Munoz DP, Fecteau JH.** Vying for dominance: dynamic interactions control visual fixation and saccadic initiation in the superior colliculus. *Prog Brain Res* 140: 3–19, 2002. doi:10.1016/S0079-6123(02)40039-8.
- Noorani I.** Towards a unifying mechanism for cancelling movements. *Philos Trans R Soc Lond B Biol Sci* 372: 20160191, 2017. doi:10.1098/rstb.2016.0191.
- Noorani I, Carpenter RH.** Antisaccades as decisions: LATER model predicts latency distributions and error responses. *Eur J Neurosci* 37: 330–338, 2013. doi:10.1111/ejn.12025.
- Noorani I, Carpenter RH.** Re-starting a neural race: anti-saccade correction. *Eur J Neurosci* 39: 159–164, 2014. doi:10.1111/ejn.12396.
- Noorani I, Carpenter RH.** Ultrafast initiation of a neural race by impending errors. *J Physiol* 593: 4471–4484, 2015. doi:10.1113/JP270842.
- Noorani I, Carpenter RH.** The LATER model of reaction time and decision. *Neurosci Biobehav Rev* 64: 229–251, 2016. doi:10.1016/j.neubiorev.2016.02.018.
- Noorani I, Gao MJ, Pearson BC, Carpenter RH.** Predicting the timing of wrong decisions with LATER. *Exp Brain Res* 209: 587–598, 2011. doi:10.1007/s00221-011-2587-1.
- Nyffeler T, Müri RM, Bucher-Ottiger Y, Pierrot-Deseilligny C, Gaymard B, Rivaud-Pechoux S.** Inhibitory control of the human dorsolateral prefrontal cortex during the anti-saccade paradigm—a transcranial magnetic stimulation study. *Eur J Neurosci* 26: 1381–1385, 2007. doi:10.1111/j.1460-9568.2007.05758.x.
- Oommen BS, Smith RM, Stahl JS.** The influence of future gaze orientation upon eye-head coupling during saccades. *Exp Brain Res* 155: 9–18, 2004. doi:10.1007/s00221-003-1694-z.
- Oommen BS, Stahl JS.** Overlapping gaze shifts reveal timing of an eye-head gate. *Exp Brain Res* 167: 276–286, 2005. doi:10.1007/s00221-005-0036-8.
- Paré M, Hanes DP.** Controlled movement processing: superior colliculus activity associated with countermanded saccades. *J Neurosci* 23: 6480–6489, 2003. doi:10.1523/JNEUROSCI.23-16-06480.2003.
- Phillips JO, Ling L, Fuchs AF, Siebold C, Plorde JJ.** Rapid horizontal gaze movement in the monkey. *J Neurophysiol* 73: 1632–1652, 1995. doi:10.1152/jn.1995.73.4.1632.
- Pouget P, Logan GD, Palmeri TJ, Boucher L, Paré M, Schall JD.** Neural basis of adaptive response time adjustment during saccade countermanding. *J Neurosci* 31: 12604–12612, 2011. doi:10.1523/JNEUROSCI.1868-11.2011.
- Pouget P, Murthy A, Stuphorn V.** Cortical control and performance monitoring of interrupting and redirecting movements. *Philos Trans R Soc Lond B Biol Sci* 372: 20160201, 2017. doi:10.1098/rstb.2016.0201.
- Prablanc C, Echallier JF, Komilis E, Jeannerod M.** Optimal response of eye and hand motor systems in pointing at a visual target. I. Spatio-temporal characteristics of eye and hand movements and their relationships when varying the amount of visual information. *Biol Cybern* 35: 113–124, 1979. doi:10.1007/BF00337436.
- Pruszynski JA, Lillcrap TP, Scott SH.** Complex spatiotemporal tuning in human upper-limb muscles. *J Neurophysiol* 103: 564–572, 2010. doi:10.1152/jn.00791.2009.
- Ramakrishnan A, Sureshbabu R, Murthy A.** Understanding how the brain changes its mind: microstimulation in the macaque frontal eye field reveals how saccade plans are changed. *J Neurosci* 32: 4457–4472, 2012. doi:10.1523/JNEUROSCI.3668-11.2012.
- Ray NJ, Jenkinson N, Brittain J, Holland P, Joint C, Nandi D, Bain PG, Yousif N, Green A, Stein JS, Aziz TZ.** The role of the subthalamic nucleus in response inhibition: evidence from deep brain stimulation for Parkinson's disease. *Neuropsychologia* 47: 2828–2834, 2009a. doi:10.1016/j.neuropsychologia.2009.06.011.
- Ray S, Pouget P, Schall JD.** Functional distinction between visuomovement and movement neurons in macaque frontal eye field during saccade countermanding. *J Neurophysiol* 102: 3091–3100, 2009b. doi:10.1152/jn.00270.2009.
- Reddi BA, Carpenter RH.** The influence of urgency on decision time. *Nat Neurosci* 3: 827–830, 2000. doi:10.1038/77739.
- Sailer U, Eggert T, Ditterich J, Straube A.** Spatial and temporal aspects of eye-hand coordination across different tasks. *Exp Brain Res* 134: 163–173, 2000. doi:10.1007/s002210000457.
- Salinas E, Stanford TR.** The countermanding task revisited: fast stimulus detection is a key determinant of psychophysical performance. *J Neurosci* 33: 5668–5685, 2013. doi:10.1523/JNEUROSCI.3977-12.2013.
- Schall JD, Godlove DC.** Current advances and pressing problems in studies of stopping. *Curr Opin Neurobiol* 22: 1012–1021, 2012. doi:10.1016/j.conb.2012.06.002.
- Schall JD, Palmeri TJ, Logan GD.** Models of inhibitory control. *Philos Trans R Soc Lond B Biol Sci* 372: 20160193, 2017. doi:10.1098/rstb.2016.0193.
- Schmidt R, Leventhal DK, Mallet N, Chen F, Berke JD.** Canceling actions involves a race between basal ganglia pathways. *Nat Neurosci* 16: 1118–1124, 2013. doi:10.1038/nn.3456.
- Song JH.** Abandoning and modifying one action plan for alternatives. *Philos Trans R Soc Lond B Biol Sci* 372: 20160195, 2017. doi:10.1098/rstb.2016.0195.
- Stevenson SA, Elsley JK, Corneil BD.** A “gap effect” on stop signal reaction times in a human saccadic countermanding task. *J Neurophysiol* 101: 580–590, 2009. doi:10.1152/jn.90891.2008.
- Stuphorn V, Schall JD.** Executive control of countermanding saccades by the supplementary eye field. *Nat Neurosci* 9: 925–931, 2006. doi:10.1038/nn1714.
- Stuphorn V, Taylor TL, Schall JD.** Performance monitoring by the supplementary eye field. *Nature* 408: 857–860, 2000. doi:10.1038/35048576.
- Suzuki M, Izawa A, Takahashi K, Yamazaki Y.** The coordination of eye, head, and arm movements during rapid gaze orienting and arm pointing. *Exp Brain Res* 184: 579–585, 2008. doi:10.1007/s00221-007-1222-7.
- Tao G, Blohm G.** Corrective response reaction times and multi-motor coordination after countermanding failures (Abstract). *J Vis* 11: 900, 2011. doi:10.1167/11.11.900.
- Tweed D, Glenn B, Vilis T.** Eye-head coordination during large gaze shifts. *J Neurophysiol* 73: 766–779, 1995. doi:10.1152/jn.1995.73.2.766.
- Verbruggen F, Logan GD.** After-effects of goal shifting and response inhibition: a comparison of the stop-change and dual-task paradigms. *Q J Exp Psychol (Hove)* 61: 1151–1159, 2008a. doi:10.1080/17470210801994971.
- Verbruggen F, Logan GD.** Response inhibition in the stop-signal paradigm. *Trends Cogn Sci* 12: 418–424, 2008b. doi:10.1016/j.tics.2008.07.005.
- Verbruggen F, Logan GD.** Models of response inhibition in the stop-signal and stop-change paradigms. *Neurosci Biobehav Rev* 33: 647–661, 2009. doi:10.1016/j.neubiorev.2008.08.014.
- Vercher JL, Magenes G, Prablanc C, Gauthier GM.** Eye-head-hand coordination in pointing at visual targets: spatial and temporal analysis. *Exp Brain Res* 99: 507–523, 1994. doi:10.1007/BF00228987.
- Zangemeister WH, Stark L.** Gaze latency: variable interactions of head and eye latency. *Exp Neurol* 75: 389–406, 1982. doi:10.1016/0014-4886(82)90169-8.